

602449

1 of 3

**AEROSPACE ELECTRICAL DIVISION**

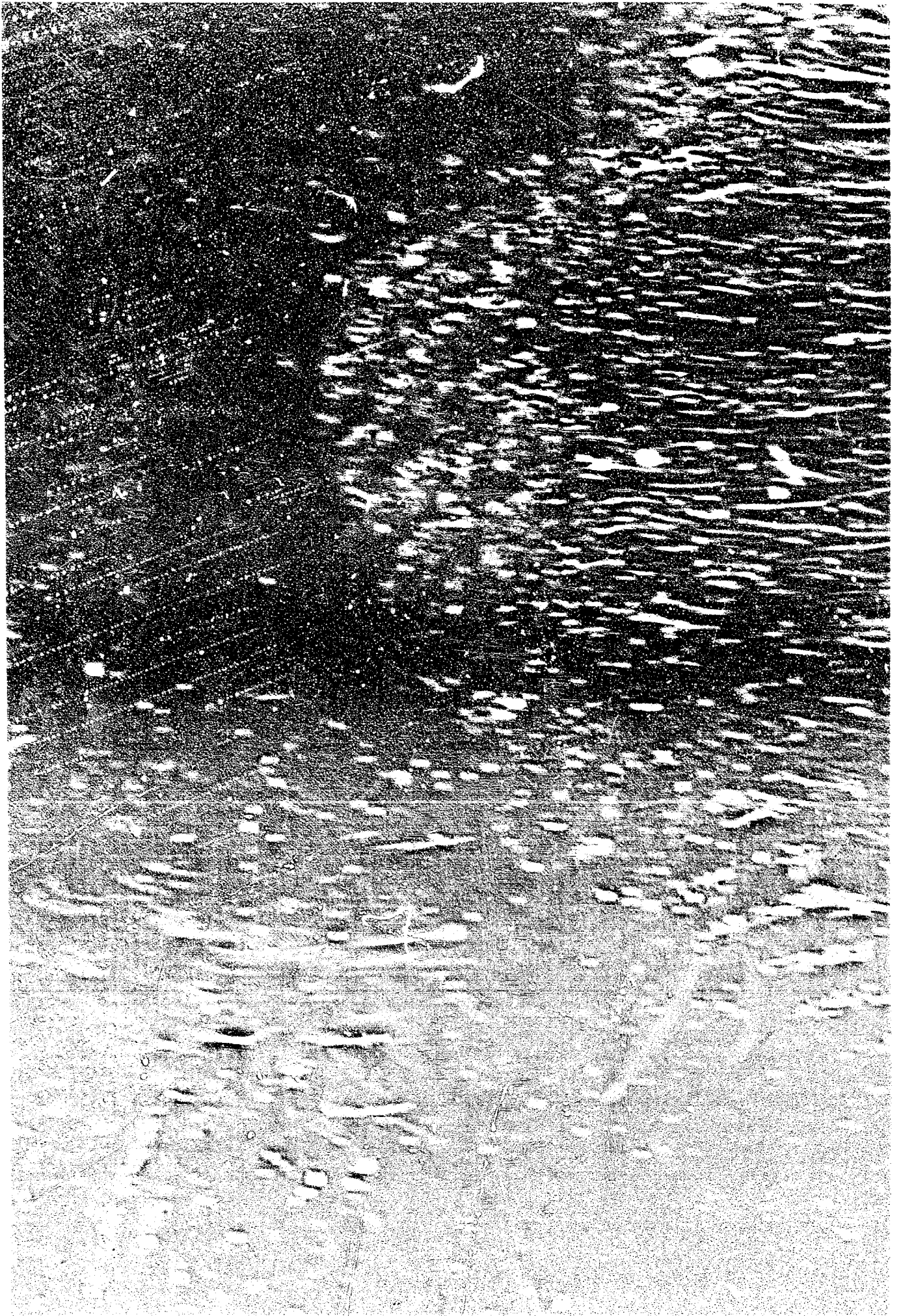
**HIGH TEMPERATURE**

**ALKALI METAL RESISTANT INSULATION**

87 p \$3.00 kc  
\$0.75 mf

**USAF Contract AF33(615)1360**  
**Project No. 8128**  
**Task No. 8128-06**

**WESTINGHOUSE ELECTRIC CORPORATION**  
**AEROSPACE ELECTRICAL DIVISION**  
**LIMA, OHIO**



WAED - 64.39.E

JULY 10, 1964

This Quarterly Report covers the period April 1, 1964 to June 30, 1964 on  
Contract AF33(615)1360, Task No. 8128-06.

PREPARED BY:

*W. H. Snavely*  
W. H. Snavely, Project Engineer

*R. E. McVay*  
R. E. McVay, Senior Engineer

*R. E. Stapleton*  
R. E. Stapleton, Senior Engineer

*R. M. Frost*  
R. M. Frost, Project Manager

*J. D. Miner*  
Approved by J. D. Miner  
Manager of Engineering

**High Temperature Alkali Metal Resistant Insulation**

**1st Quarterly Progress Report  
Contract AF33(615)1360, Task No. 8128-06**

**July 10, 1964**

**Westinghouse Electric Corporation  
Aerospace Electrical Division  
Lima, Ohio**

## NOTICE

The work covered by this report was accomplished under Air Force Contract AF33(615)1360, but this report is being published and distributed prior to Air Force review. The publication of this report, therefore, does not constitute approval by the Air Force of the findings and conclusions contained herein. It is published for the exchange and stimulation of ideas.

## FOREWARD

This 1st Quarterly Report is submitted by the Aerospace Electrical Division, Westinghouse Electric Corporation, Lima, Ohio, on Air Force Contract AF33(615)1360, Project No. 8128, Task No. 8128-06 High Temperature Alkali Metal Resistant Insulation. The contract is administered by the Air Force Aero-Propulsion Laboratory, Research and Technology Division, Wright-Patterson Air Force Base, Dayton, Ohio. Mr. Lester Schott is project engineer for APIP on this contract.

The work described in this report was done by personnel in the Materials Engineering and Research and Development Groups at Westinghouse AED, Lima, Ohio.

ABSTRACT

This report covers the progress during the first quarter on Air Force Contract AF33(615)1360.

Materials <sup>WFRT</sup> ~~have been~~ selected for 850<sup>e</sup>C potassium vapor exposure.

A transformer ~~has been~~ <sup>designed</sup> and selected as a test device to determine the combined effect of 600<sup>e</sup>C potassium vapor, fluctuating magnetic fields and high a-c voltage (~~1000 VAC~~) on insulators, potting compounds, magnetic materials, and electrical conductors. Potassium vapor corrosion tests are in progress on the materials that will be used in the final test transformer. Ceramic to metal seal development is being studied extensively as terminal seals for electrical feed throughs will be needed for electrical testing in potassium vapor at elevated temperatures. ( )

## TABLE OF CONTENTS

Section		Page
I	INTRODUCTION .....	1
II	SUMMARY OF WORK PERFORMED AND MAJOR RESULTS.	2
III	EXPERIMENTAL WORK .....	4
	3.1 Potassium Vapor Exposure .....	4
	3.1.1 Improved Capsule Load Procedure .....	4
	3.2 Electrical Conductors .....	6
	3.2.1 Conductor Description .....	6
	3.2.2 Conductivity Measurements - Elevated Temperatures .....	6
	3.3 Theoretical Considerations of Alkali Metal Corrosion Effects .....	7
	3.3.1 Ceramic-Metal Interfaces and Thermodynamic Calculations .....	7
	3.4 Insulation Resistivity Measurements .....	22
	3.4.1 Test Fixture .....	22
	3.4.2 Sample Electroding .....	22
	3.5 Plasma Sprayed Interlaminar Insulation .....	24
	3.5.1 Structure of High Purity $Al_2O_3$ and $Y_2O_3$ Coatings .....	24
	3.6 Processed Insulators .....	28
	3.6.1 High Alumina Ball Mill .....	28
	3.6.2 Inorganic Fluoride Insulation .....	32

75

## TABLE OF CONTENTS (Cont.)

Section		Page
3.7	Pressure Sintered Ceramic - Metal Composites and Hermetic Seals .....	33
	3.7.1 Hot Pressing Rig .....	33
3.8	Ceramic to Metal Seals .....	34
	3.8.1 Active Metal Brazing .....	34
	3.8.2 Conventional Molybdenum - Manganese (80 - 20%) Metallizing .....	35
	3.8.3 Vapor Decomposition of a Tungsten Halide Complex .....	35
3.9	850 C Potassium Vapor Exposure - Active Metal Brazing Alloys .....	35
	3.9.1 Ten Active Metal Brazing Alloys .....	35
3.10	Magnetic Materials .....	35
	3.10.1 Materials Selection .....	35
	3.10.2 Magnetic Testing .....	36
	3.10.3 Preliminary Evaluation of Magnetic Tests .	38
3.11	Special Transformer .....	48
	3.11.1 Description and Design .....	48
IV	PROGRAM FOR NEXT QUARTER .....	52
	4.1 Potassium Vapor Corrosion Effects .....	52
	4.2 Magnetic Materials .....	52
	4.3 Conductors .....	52

**TABLE OF CONTENTS (Cont.)**

<b>Section</b>		<b>Page</b>
4.4	Ceramic Materials .....	53
4.5	Transformer Fabrication .....	53
4.6	Plasma-Arc Spraying of Ceramics .....	53
V	REFERENCES .....	53
	APPENDIX A .....	56

## LIST OF ILLUSTRATIONS

Figure		Page
1	View of Vacuum - Inert Atmosphere Glove Box and Capsule Loading Assembly .....	8
2	Electrical Resistivity of Silver Versus Temperature .....	9
3	Electrical Resistivity of 70% Columbium Clad Dispersion Strengthened Copper Versus Temperature .....	10
4	Electrical Resistivity Versus Temperature of 70% Columbium Clad Zirconium Copper .....	11
5	Electrical Resistivity of 70% Columbium Clad Silver Versus Temperature .....	12
6	Electrical Resistivity of OFHC Copper Compared with 28% Nickel Clad Silver .....	13
7	Spring Loaded Stainless Steel Fixtures for Resistivity Measurements .....	23
8	Plasma Sprayed Linde A on Hiperco, 100 Amps Arc Current (500 X Magnification) .....	25
9	Plasma Sprayed Linde A on Hiperco, 600 Amps Acr Current (500 X Magnification) .....	25
10	E Core Hiperco Lamination Sprayed Linde A, 600 Amps (500 X Magnification) .....	25
11	Plasma Sprayed Linde A, 650 Amps Arc Current (500 X Magnification) .....	26

## LIST OF ILLUSTRATIONS (Cont.)

Figure		Page
12	Plasma Sprayed Linde A, 500 Amps Arc Current (1000 X Magnification) .....	26
13	Yttrium Oxide Plasma Sprayed on E Core Hiperco 600 Amps (500 X Magnification) .....	26
14	High Purity Alumina Ball Mill Lining: Triangle RR (99.7% $\text{Al}_2\text{O}_3$ ) .....	29
15	High Purity Alumina (Alite 610) Prereacted to Achieve Large Particle Sieze Material (200 X Magnification) .....	31
16	Same Material as Shown in Figure 15 Except Ball Milled for Approximately 90 Hours in Mill Shown in Figure 14 (200 X Magnification) .....	31
17	Rowland Ring Laminations Used in Magnetic Testing .....	37
18	Core Loss of 0.008" Hiperco 27, Mylar Insulated .....	40
19	Apparent Core Loss of 0.008" Hiperco 27, Mylar Insulated..	41
20	Core Loss of 0.008" Hiperco 27, $\text{Al}_2\text{O}_3$ (99.99%) Insulated ..	42
21	Apparent Core Loss 0.008" Hiperco 27, $\text{Al}_2\text{O}_3$ (99.99%) Insulated .....	43
22	Core Loss of 0.008" Armco Ingot Iron, Mylar Insulated ....	44
23	Apparent Core Loss of 0.008" Armco Ingot Iron, Mylar Insulated .....	45

LIST OF ILLUSTRATIONS (Cont.)

Figure		Page
24	Core Loss of 0.006" Cubex, Mylar Insulated .....	46
25	Apparent Core Loss of 0.006" Cubex, Mylar Insulated .....	47
26	Top and End View of Special Transformer Using Ceramic Spool Insulators of Alite A-610 Material (Actual Size) .....	49
27	Ceramic Ground Insulator Made of Alite A-610 (99.0% Al <sub>2</sub> O <sub>3</sub> .1% MgO) .....	50
28	Ceramic Coil Form Measurements .....	51

## LIST OF TABLES

Number		Page
I	Materials on Test in 850 C Potassium .....	5
II	Free Energies of Formation at 850 C (Reference 3, 4) - in Order of Increasing Values for Oxides and Fluorides (Per Gram Mole of Oxygen or Florine) .....	17
III	Active Alloys - Candidate Systems .....	21
IV	Core Lose Separation Data .....	39

I.

## INTRODUCTION

This report covers the first quarter from April 1, 1964 to July 1, 1964 on Air Force Contract AF33(615)1360, High Temperature Alkali Metal Insulation.

The program was initiated to investigate the effect of 600-850 C potassium vapor on selected materials in an electrical test device. The test device is a transformer designed to operate in potassium vapor at 600 C. Various voltages to 1000 VAC and frequencies to 32000 cps are to be applied to the primary windings. Fifty amperes at thirty-two volts will be the output of the secondary winding. The transformer is to be operated at these electrical test conditions for 500 hours. Examination of the materials after the test period will be done to determine the effect of the combined environmental test conditions.

## II. SUMMARY OF WORK PERFORMED AND MAJOR RESULTS

1. Materials have been selected and ordered from various manufacturers for corrosion testing in potassium vapor at 850°C.

2. Ten ceramic insulator and insulation samples are currently being exposed to potassium vapor at 850°C. Two of these samples are magnetic material (Hiperco 27) plasma arc sprayed with sub micron particle size alumina (99.99%) and yttria (99.9%). The total coating thickness of these ceramics on the 0.008" thick Hiperco 27 is  $\sim 0.0008$ ".

3. 70% Columbium clad CuFo (beryllium oxide dispersion strengthened copper), 70% columbium clad Zr. copper, 70% columbium clad silver and 28% nickel clad silver conductors in AWG No. 22 size have been received. Resistivity measurements have been performed on these clad conductors at temperatures up to 1700 F. Calculated and experimental results show a lower volume percent. Columbium cladding is needed to stay below the 150% resistivity of OFHC copper requirement.

4. Rowland ring specimens for magnetic testing of Hiperco 27, Cubex, and Armco Iron have been punched. Magnetic test data has been obtained for these materials at room temperature.

5. Apparatus to make hot pressed ceramics is being assembled. A study of the effect, due to varying the current density of the plasma-arc on sub micron size alumina particle spraying, has been completed. The results indicate a preferred current density for the existing plasma-spray apparatus is 550-600 amperes. A special sub micron size particle feed apparatus for the plasma spray equipment has been designed, built, and is working very well.

6. A special alumina (99.9%) ball mill has been constructed to grind ceramics and reduce the particle size with a minimum pick up of silica. Experiments show that silica pick up is  $\sim 0.02\%$  using this ball mill. (Commercial ball mills using 85% ceramic balls may impart 0.50 - 1.0% silica to a high purity ceramic, such as 99.9% alumina.)

7. Several approaches to the problem of obtaining a ceramic-to-metal seal that will enable the electrical tests in potassium vapor to be completed are being investigated. The seals made by conventional molybdenum-manganese and active metal brazing techniques are being evaluated by exposure to 600-850 C potassium vapor.

8. A special transformer design has been completed and materials are on order to construct it. The transformer laminations of Hiperco 27, Cubex, and Armco Iron have been fabricated. 28% Nickel clad silver conductor in wire sizes 22 and 6 AWG has been received from the Sylvania Special Products Division in Warren, Pa. Special ceramic spools to be used as transformer coil forms are on order from the Alite Division of U.S. Stoneware in Orrville, Ohio.

### III.

## EXPERIMENTAL WORK

### 3.1 Potassium Vapor Exposure

The materials listed in Table I are currently being exposed to potassium vapor at 850 C. The technique used to prepare the material and capsules was similar to that described in Air Force Report No. APL-TDR-64-42.

#### 3.1.1 Improved Capsule Loading Procedure

The method of preparing and loading potassium vapor exposure test capsules has been modified. The exposure capsules are fabricated of 0.5" type 321 stainless steel tubing 8" long with a 0.5" swagelok connection at the open end. The other end is crimp sealed and TIG welded. The potassium and sample are placed in the capsules after a thorough cleaning and baking out procedure. Capsules are then connected to a 0.75" vacuum line ( $8 \times 10^{-5}$  torr) running into an inert atmosphere glove box. After a time interval of  $\sim 20$  minutes, the capsules are crimped with a hydraulic crimping tool inside the vacuum-inert atmosphere glove box, cut from the line and welded by use of a welding electrode inside the inert atmosphere box. This assembly is shown in Figure I.

**TABLE I**

**Materials on Test in 850 C Potassium Vapor**

1. Strontium Fluoride, single crystal, Semi Elements Inc.
2. Calcium Fluoride, single crystal, Semi Elements Inc.
3. Barium Fluoride, single crystal, Semi Elements Inc.
4. Calcium Oxide, single crystal, Semi Elements Inc.
5. Boron Nitride, pyrolytically deposited, High Temperature Materials, Inc.
6. Triangle RR, 99.7%  $\text{Al}_2\text{O}_3$ , Morgan Refractories
7. A-610 (99.0%  $\text{Al}_2\text{O}_3$ . 1%  $\text{MgO}$ ) Alite Division of U. S. Stoneware
8. Tungsten-vapor deposited on high purity alumina, Sylvania Chemical & Metallurgical
9. Yttrium Oxide, plasma-arc sprayed on 8 mil Hiperco 27 substrate
10. Linde A (0.3 micron size  $\text{Al}_2\text{O}_3$ ) on 8 mil Hiperco 27 substrate

## 3.2 Electrical Conductors

### 3.2.1 Conductor Description

The following conductors were ordered and obtained for evaluation.

1. 28% Nickel clad silver, Sylvania Special Products Div., Warren, Pa.  
No. 22 & No. 6 AWG
2. Columbium clad dispersion strengthened copper, Westinghouse Blairsville  
No. 22 AWG Div., Blairsville, Pa.
3. Columbium clad Zr-copper, Westinghouse Blairsville Div., Blairsville,  
Pa.
4. Columbium clad silver, Westinghouse Blairsville Div., Blairsville, Pa.

The 28% nickel clad silver conductor had previously been tested for high temperature electrical conductivity and 500-hour potassium vapor exposure at 850 C.

This nickel clad conductor was chosen as a conductor to wind the first transformer for these preceding reasons.

The nickel clad silver has some strength limitations at elevated temperature, consequently, columbium clad strengthened copper and silver conductors were obtained to measure their conductivity or resistivity at temperatures to 1700 F.

### 3.2.2 Conductivity Measurements - Elevated Temperatures

Columbium clad conductors were made in No. 22 AWG; however the cladding thickness was 70 volume percent. Theoretically, this 70% thickness is outside the 150% resistivity of OFHC copper specified by the contract.

However, resistivity measurements were conducted on the three columbium clad conductors to observe flatness characteristics. Resistance measurements were made on these conductors in an inert gas atmosphere resistance heated tube furnace using a Kelvin bridge and four point method. Resistivity versus temperature data are shown for silver at various temperatures compared to a standard set of resistivity data for silver. Figure 2 illustrates the two sets of data and these data serve as a check on experimental technique and instrumentation. Figures 3, 4, 5 and 6 show resistivity versus temperature data for 70% columbium-clad, dispersion-strengthened copper (Cu Fo core by Handy and Harmon), 70% columbium clad zirconium copper (0.15% Zr, > 99.5% Cu), 70% columbium clad silver and 28% nickel clad silver. The size of all these conductors was 0.0254" (No. 22 AWG). Calculated values of resistivity for a 28% columbium clad conductor are shown in Appendix A.

### 3.3 Theoretical Considerations of Alkali Metal Corrosion Effects

#### 3.3.1 Ceramic-Metal Interfaces and Thermodynamic Calculations.

The solution to the problem of bonding two dissimilar materials together involves finding a mechanism whereby the interface energy can be lowered. The interface energy between two phases is always less than the sum of the separate surface energies of the two phases since there is always some energy of attraction. Liquid metals generally have much higher surface energies than ceramic oxides, and the interface energy is high; therefore, wetting does not occur. The interface energy between two chemically similar phases

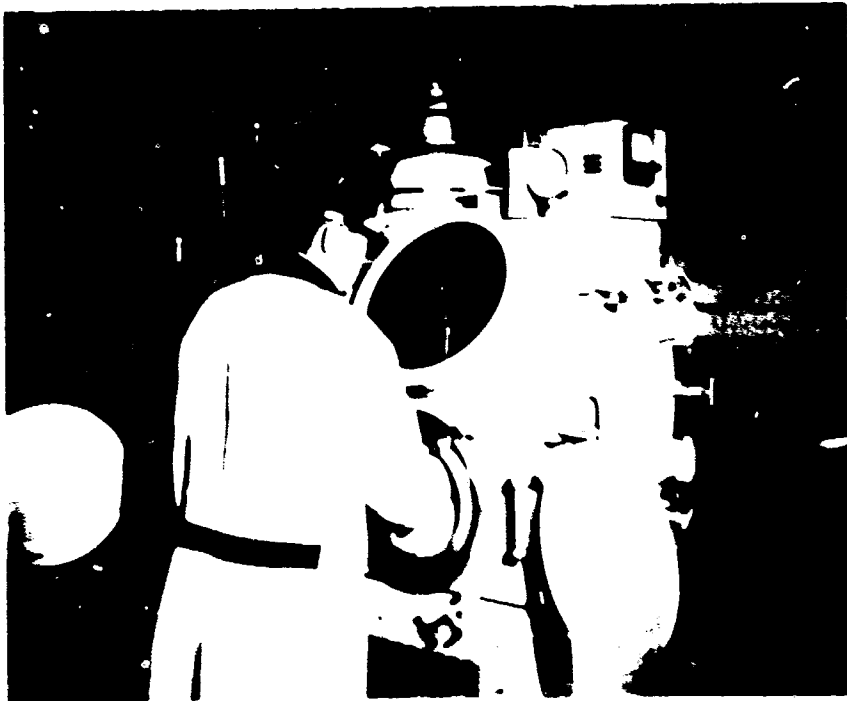
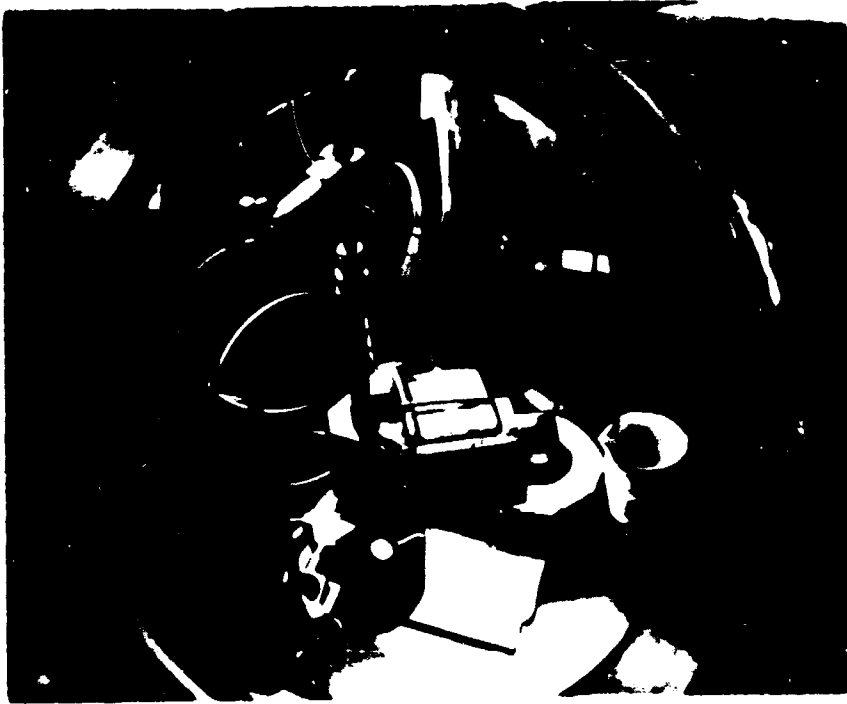


Figure 1. View of Vacuum - Inert Atmosphere Glove Box  
and Capsule Loading Assembly

Silver - Pure

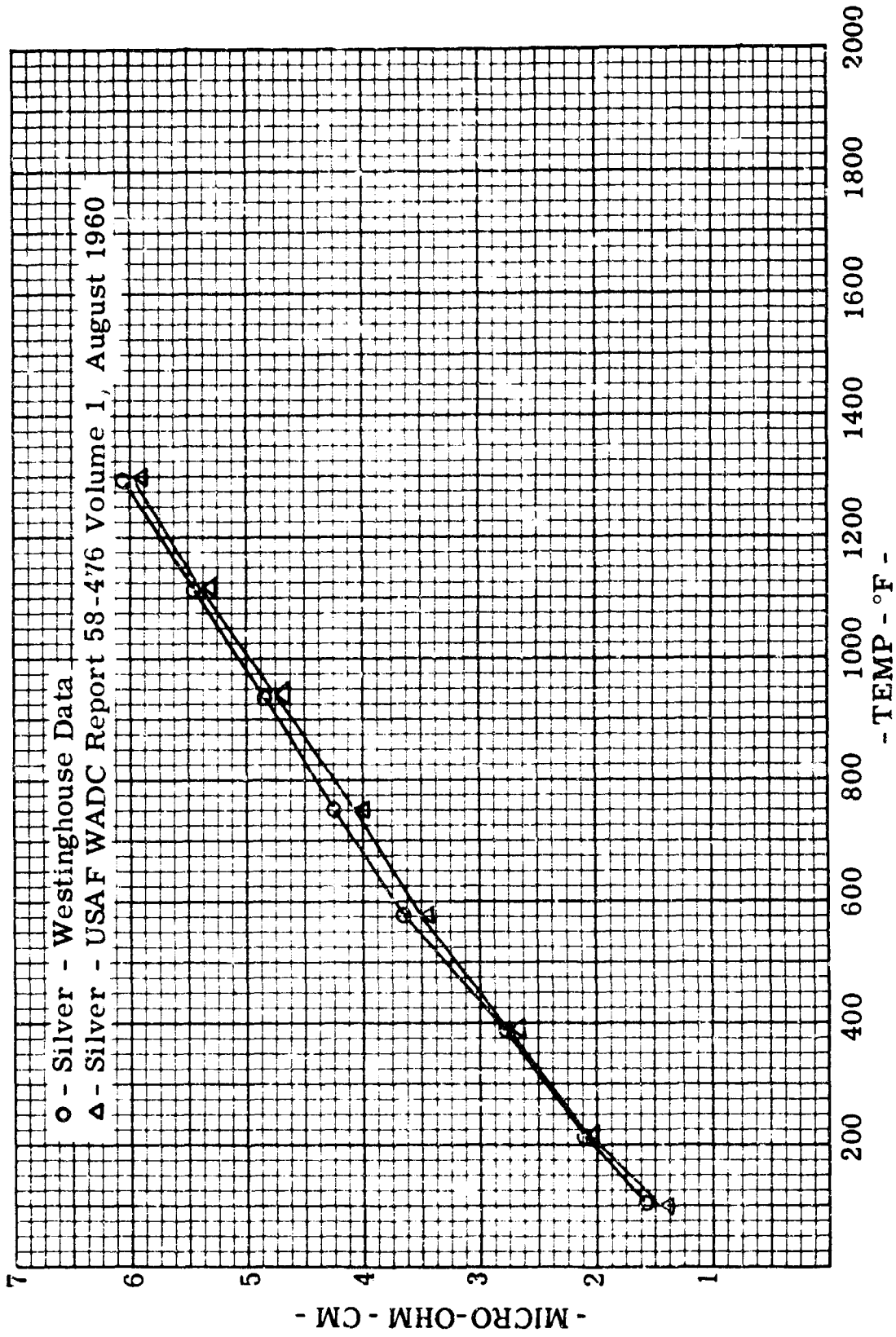


Figure 2. Electrical Resistivity of Silver Versus Temperature

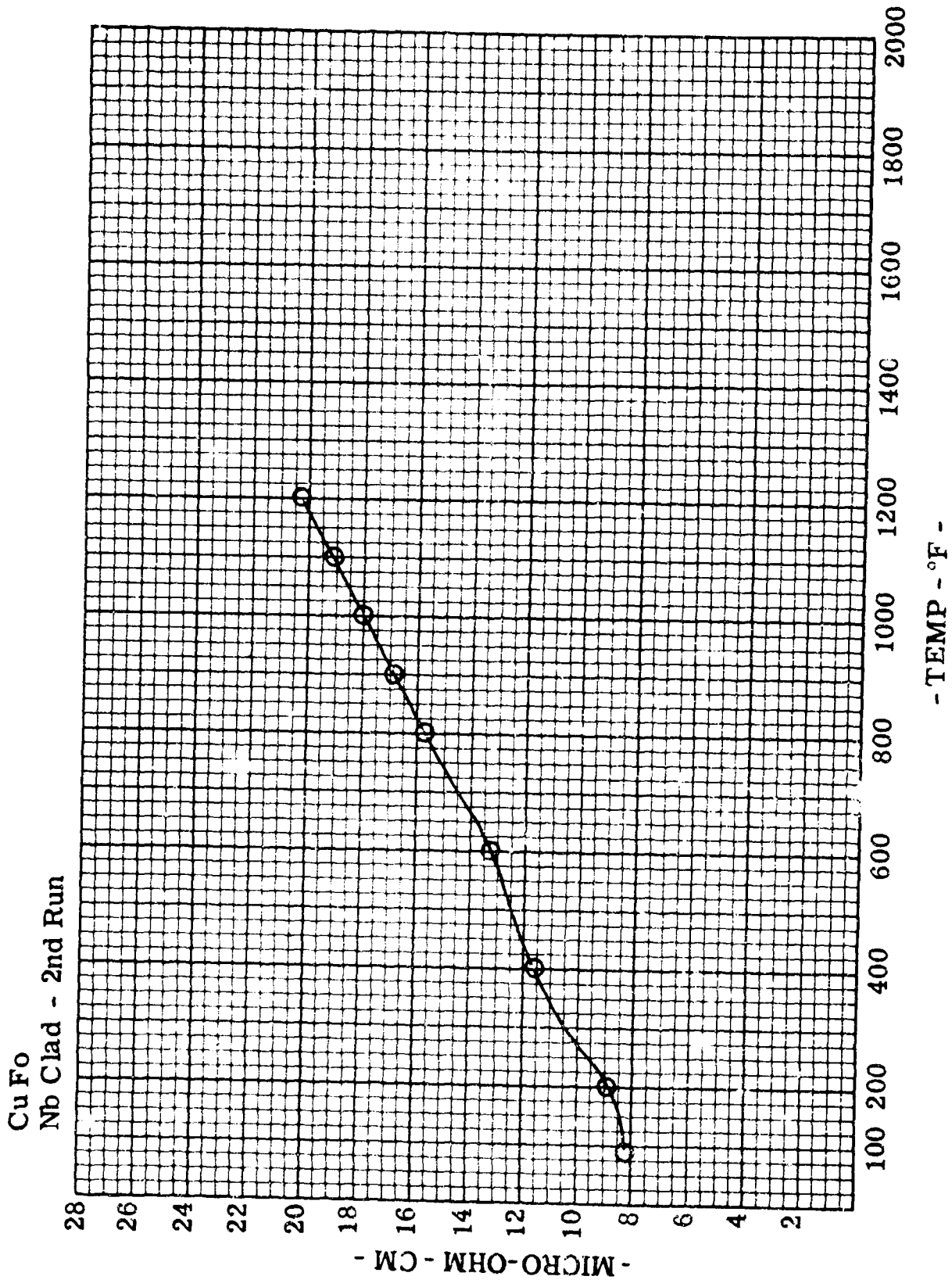


Figure 3. Electrical Resistivity of 70% Columbium Clad Dispersion Strengthened Copper Versus Temperature

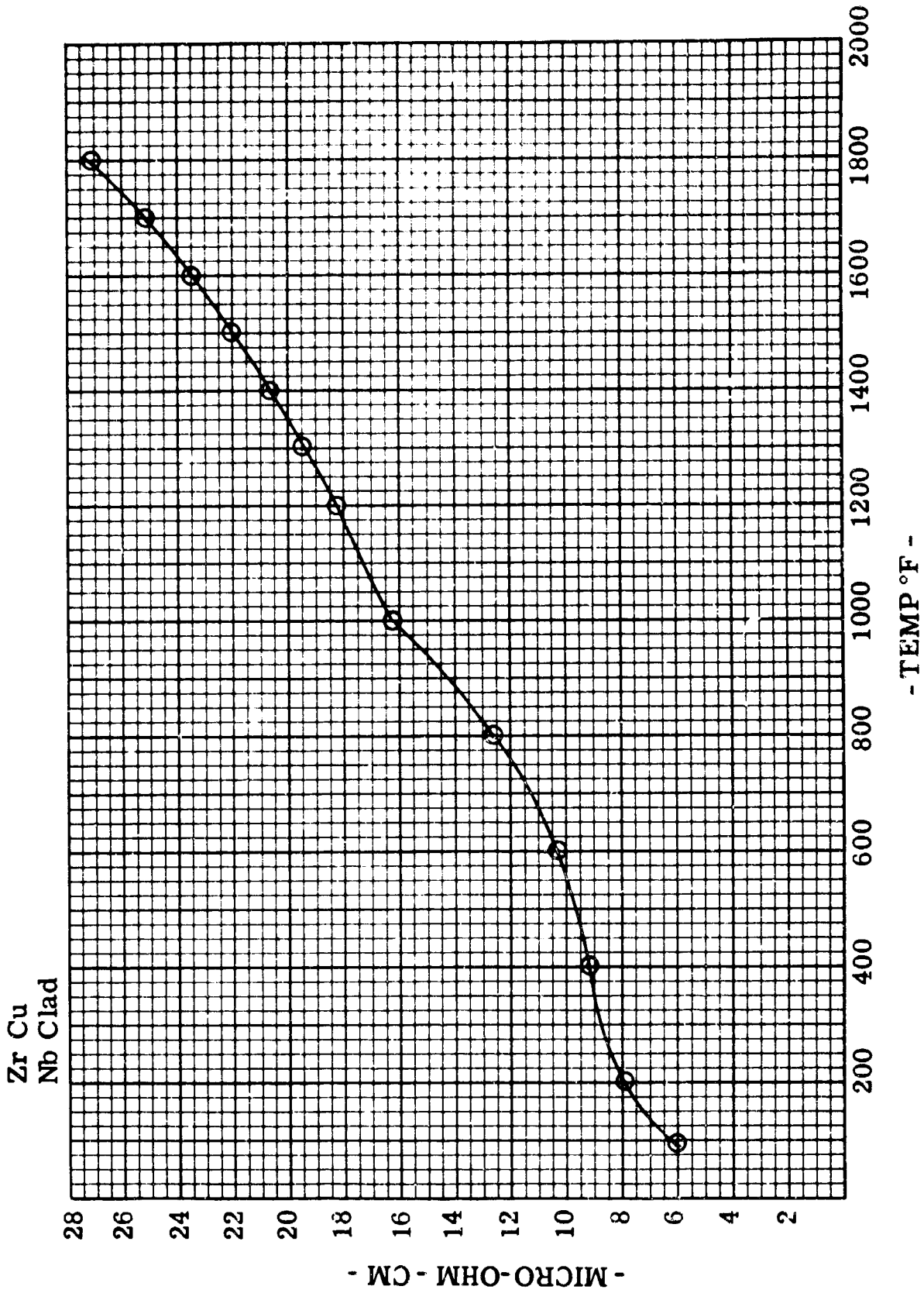


Figure 4. Electrical Resistivity Versus Temperature of 70% Columbium Clad Zirconium Copper

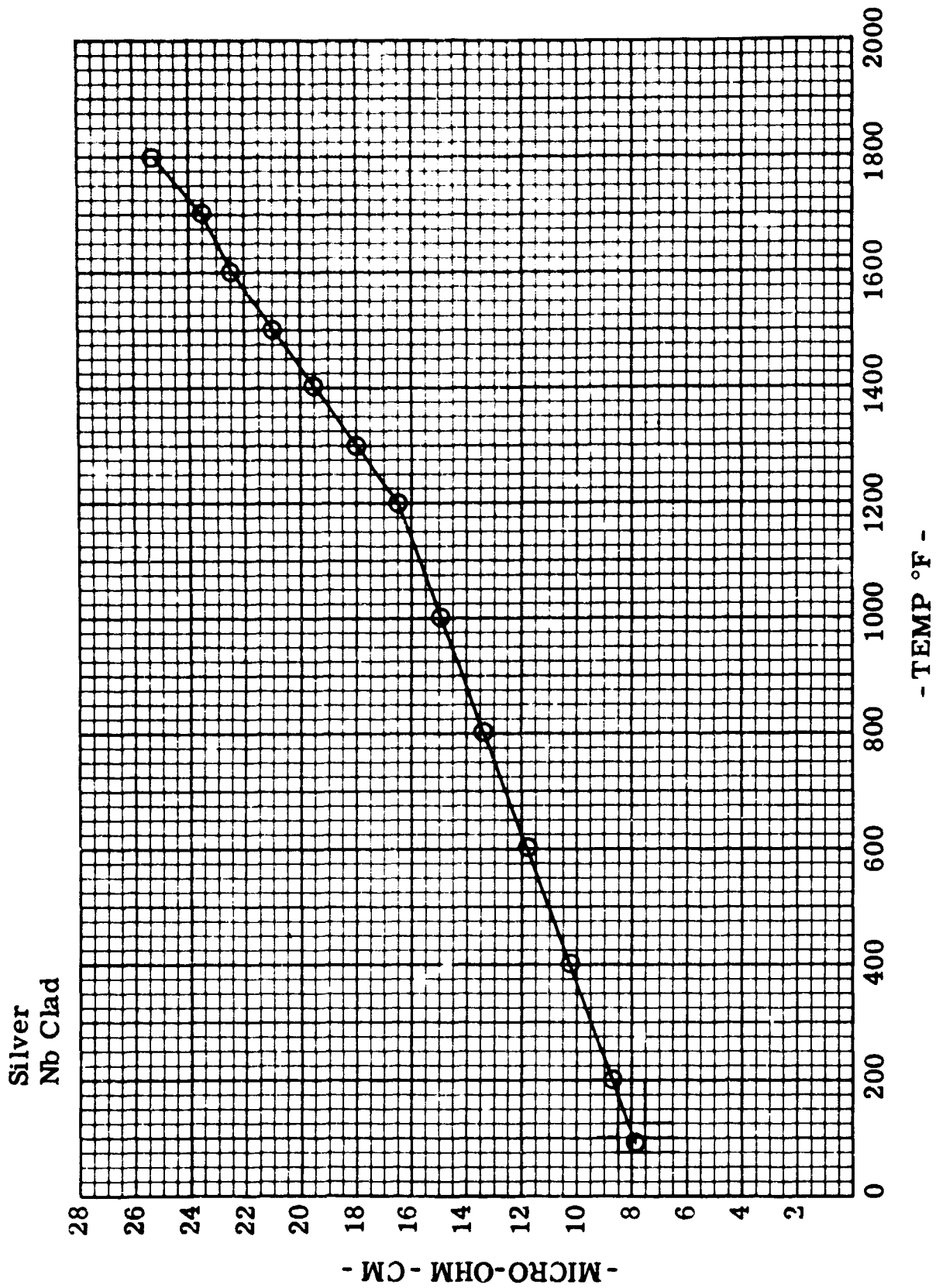


Figure 5. Electrical Resistivity of 70% Columbium Clad Silver Versus Temperature

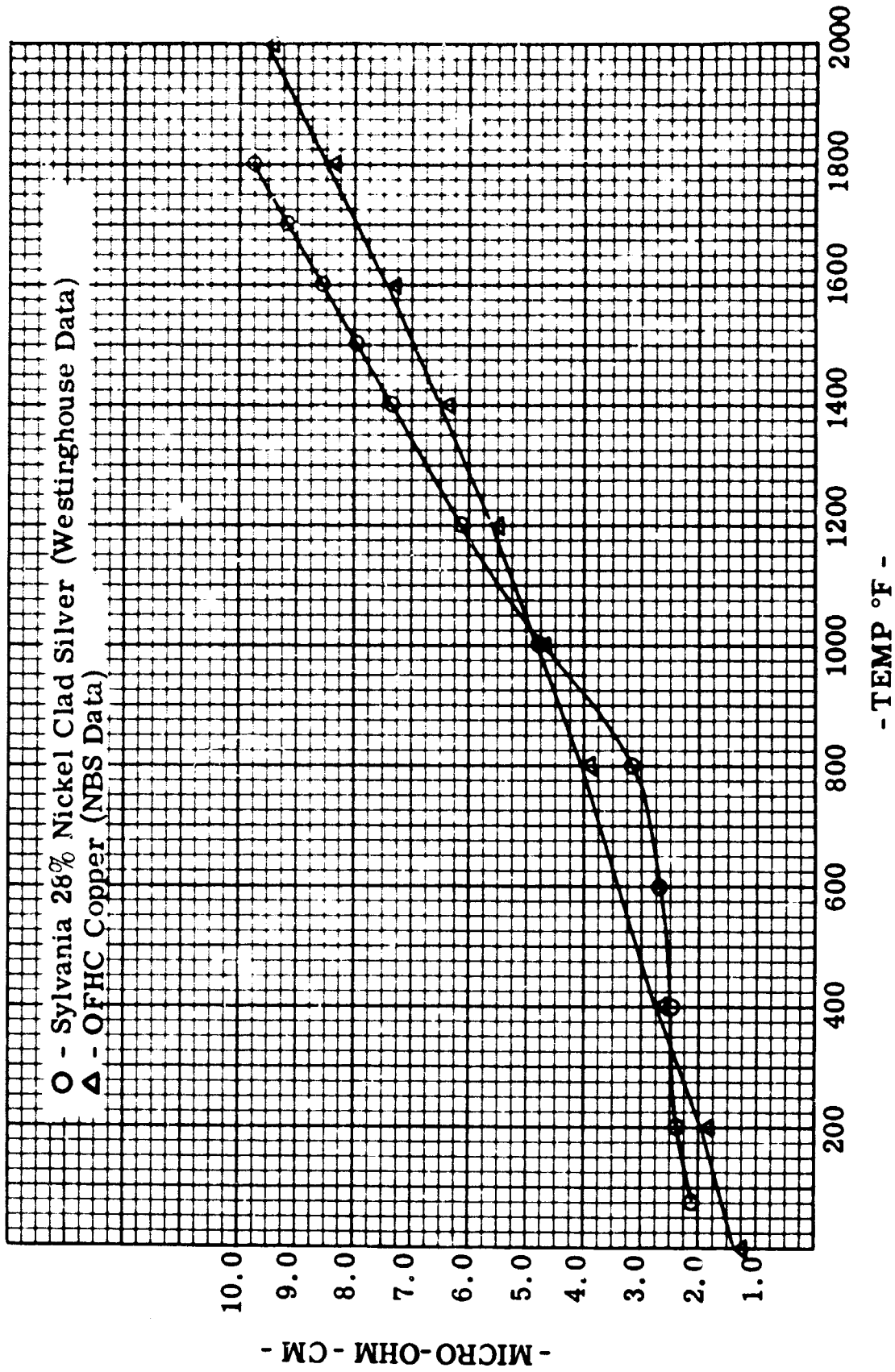


Figure 6. Electrical Resistivity of OFHC Copper Compared with 28% Nickel Clad Silver

(metal-metal or oxide-oxide) is generally low, indicating the energy of attraction is high according to the following:

$$(1) \quad W = \gamma (1 + \cos \theta)$$

where

$W$  = work of adhesion (work against surface forces required to separate the metal and ceramic), ergs/cm<sup>2</sup>

$\theta$  = contact angle measured through the liquid phase

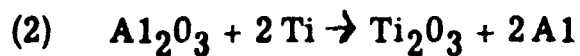
$\gamma$  = surface tension of the liquid phase

Humench and Kingerly<sup>(1)</sup> conclude that wettability and work of adhesion are increased by low surface tension, interfacial reaction and high metal-oxide bond strengths. Other important considerations are: 1) relative thermal expansion of the phases, 2) their bulk strengths, 3) surface roughness, 4) size and shape of the interface.

No one system of bonding is capable of meeting all design applications. After considering the fundamentals governing adhesion between ceramics and metals, it becomes apparent that the interface composition will play a significant part in the overall corrosion resistance and serviceability of the ceramic seal. The composition and structure of the interface will depend on a number of processing variables such as temperature, time, and gas phase composition as well as the composition and structure of the reacting liquid and solid phases. If the individual ceramic and metal materials selected have demonstrated resistance

to alkali metals, then one cannot conclude that a combination of these materials reacted to form a hermetic seal will provide a corrosion resistant seal.

Consider the reaction between a high purity sapphire crystal ( $\text{Al}_2\text{O}_3$ ) and a nickel alloy containing titanium. Definite evidence of the existence of an interface composition  $\alpha$ - $\text{Ti}_2\text{O}_3$  is reported by W. M. Armstrong<sup>(2)</sup> et al. The authors postulate the following reactions:



The compound  $\text{Ti}_2\text{O}_3$  is crystallographically similar to  $\alpha$ - $\text{Al}_2\text{O}_3$ ; therefore, there is little or no strain between the phases. The authors conclude that bonding occurs by the formation and reaction of an excess solute (titanium) concentration at the metal-ceramic interface. This concentration can be calculated using Gibbs absorption equation:

$$(3) \quad \sigma = \frac{-d\gamma}{RT \ln c}$$

where

$\sigma$  = excess surface concentration of solute

$\gamma$  = surface tension

R = gas constant

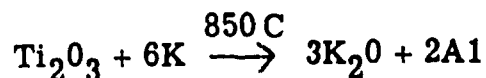
T = absolute temperature

C = bulk concentration of solute

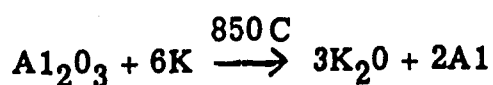
A general rule for adsorption in a multicomponent system is: 1) if the solute has a lower surface tension than the solvent the solute will be concentrated in the surface layer, 2) if the surface tension of the solute is larger, then the solute

is driven as far as possible into the interior. The reason being that molecules have different force fields and those with greater fields of force pass into the interior of the phase and those with smaller fields remain at the surface because their intrinsic free energy is lower.

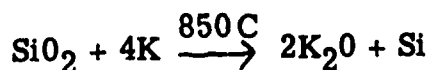
If one accepts the findings of Armstrong et al, then we are concerned with the relative corrosion resistance of the  $Ti_2O_3$  phase in the system of  $Al_2O_3$  - Nickel Titanium alloys. Table II shows a listing of the free energies of formation at 850 C of a number of oxides. For the reaction:



The free energy change is large and positive (+148 K cal). Similarly for the reaction:



The free energy change is (+175 K cal). One would conclude, therefore, that neither reaction would occur. Also, for the reaction:



A free energy change calculation also gives a positive value (+67 K cal). But this value is about 2-1/2 times less positive than the value computed from  $Al_2O_3$ . Therefore, in terms of relative stability in K vapor at 850 C, one could arrange these oxides in order of decreasing stability i.e.  $Al_2O_3 < Ti_2O_3 < SiO_2$ .

TABLE II (Sheet 1 of 2)

Free Energies of Formation at 850 C (References 3, 4) - in Order  
of Increasing Values for Oxides and Fluorides  
(Per Gram Mole of Oxygen or Florine)

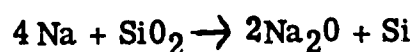
Oxide	Free Energy of Formation Kcal at 850 C	Fluorides	Free Energy of Formation Kcal at 850 C
2 Cu O	-28		
Pb O	-57		
2/3 Mo O <sub>3</sub>	-74 at 800 C		
Ge O <sub>2</sub>	-78		
Su O <sub>2</sub>	-88		
2/3 Wo <sub>3</sub>	-90		
2 K <sub>2</sub> O	-93		
2 Kn O	-110		
2/3 Cr <sub>2</sub> O <sub>3</sub>	-131		
2/5 Cb <sub>2</sub> O <sub>5</sub>	-133		
2 Mn O	-144		
Ta <sub>2</sub> O <sub>5</sub>	-146		
2/3 V <sub>2</sub> O <sub>3</sub>	-150		
Si O <sub>2</sub>	-160		
Ti O <sub>2</sub>	-175		
2/3 Ti <sub>2</sub> O <sub>3</sub>	-192		
2 Ti O	-195		
2/3 Al <sub>2</sub> O <sub>3</sub>	-210		

TABLE II (Sheet 2 of 2)

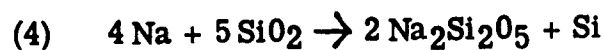
Free Energies of Formation at 850 C (Reference 3, 4) - in Order  
of Increasing Values for Oxides and Fluorides  
(Per Gram Mole of Oxygen or Florine)

Oxide	Free Energy of Formation Kcal at 850 C	Fluorides	Free Energy of Formation Kcal at 850 C
Zr O <sub>2</sub>	-211	Al F <sub>3</sub>	-178
2 Ba O	-215		
V O <sub>2</sub>	-221	2K F	-220
Sr O	-228	Mg F <sub>2</sub>	-222
2 Mg O	-228		
2 Be O	-242	Y F <sub>3</sub>	-230
Th O <sub>2</sub>	-247	2/3 La F <sub>3</sub>	-243
2 Co O	-248	Ca F <sub>2</sub>	-250
2/3 La <sub>2</sub> O <sub>3</sub>	-240	Sr F <sub>2</sub>	-250

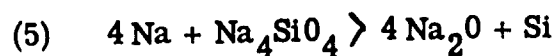
Previous work by Westinghouse on the SPUR Program has resulted in the conclusion that small amounts of  $\text{SiO}_2$  in alumina ceramics can promote corrosion in K vapor at 1100 F. In addition, the work of C. A. Elyard and H. Rawson<sup>(5)</sup> further substantiates these findings. These investigators studied the effects of Na vapor at temperatures up to 450 C on a number of simple glass compositions. They interpret their results partly on the basis of available thermodynamic data such as that shown in Table II. For example, they calculate a free-energy change at 400 C of +25 K cal for the reaction:



But, they conclude that the  $\text{Na}_2\text{O}$  formed by the above reaction will react with excess silica to form sodium disilicate. They eventually arrive at a negative free-energy value (- 107 K cal) for the reaction:



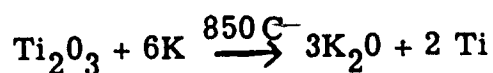
Therefore, the reaction as a whole is negative and the reduction of silica by sodium would be expected. Further consideration of the reaction between sodium and sodium orthosilicate:



gives a large and positive free energy change (+126 K cal) indicating this reaction is not favored. These investigators then postulate the following reaction sequence. Sodium first reacts to form a silicate richest in sodium ( $\text{Na}_4\text{SiO}_4$ ). This compound

will not be attacked by Na (equation 5) and will act as a barrier layer. However, this silicate will interact with the underlaying glass (by Na<sub>2</sub>O diffusion). The diffusion of Na<sub>2</sub>O will be determined by the concentration gradient; i. e. if a pure silica glass is considered, the diffusion rate will be rapid.

The foregoing has been presented in some detail to illustrate a possible analytical approach to a very complex problem area. A comparison of the findings and conclusions of Elyard and Rawson with that of Armstrong and the calculation made for the free energy change (+ 148 K cal) for the reaction.



would indicate that a nickel-titanium-alumina seal would be a satisfactory selection for further study. This system has, in fact, withstood potassium vapor at 1100 F in tests conducted at Westinghouse.

A number of other active alloy systems are presently being studied. Some of these are listed in Table III. Other factors besides surface energy considerations and corrosion resistances must also be considered. These include:

- 1) alloy ductility and embrittlement,
- 2) compatibility with metal structural parts (columbium, zirconium, etc.) and
- 3) fabrication difficulties; i. e. brazing temperatures, atmospheres, fixturing, etc.

TABLE III

## Active Alloys - Candidate Systems

Alloy	MP	
Ni - Ti Eutectic	1050 C	72% Ti, 28% Ni
Zr, Fe, V	1300 C	67% Zr, 4% Fe, 29% V
Zr, Nb, V	1280 C	60% Zr, 15% Nb, 25% V
Ti, Zr, Be	1050 C	48% Zr, 48% Ti, 4% Be
Ti, V, Mo	1250 C	63% Ti, 27% V, 10% Mo
Ti, Fe, V	1280 C	63% Ti, 27% Fe, 10% V
Ti, Nb, V	1250 C	68% Ti, 4% Nb, 28% V
Zr, Nb, Be	1050 C	75% Zr, 19% Nb, 6% Be
Ti, Zr, Nb, V	1000 C	46% Ti, 46% Zr, 4% Nb, 4% V
Ti, Zr, Fe, Mo	1200 C	62% Ti, 4% Zr, 26% Fe, 8% Mo
Zr, Be	980 C	95% Zr, 5% Be

### 3.4 Insulation Resistivity Measurements

#### 3.4.1 Test Fixture

A stainless steel, spring loaded, fixture has been designed and fabricated. The fixture will permit resistivity measurements and voltage breakdown tests to be made on insulation samples in an inert atmosphere at temperatures up to 850C. Test samples up to 3/4 inches in diameter can be used. With suitable electroding, it will be possible to measure both volume and surface resistivity during one temperature excursion.

The fixture shown in Figure 7 was assembled using machined and fired lava as temporary support and spacer insulators. Several trial runs were made in a tube furnace with flowing argon at temperatures up to 850C to check out procedures and equipment. Difficulties were experienced in obtaining high resistance readings at low temperatures and satisfactory reproducibility was not obtained. These problems are primarily due to moisture absorption in the porous lava spacers. Lava insulators are presently being replaced with high fired alumina material. Alumina was not used initially because of the necessity to secure special diamond tooling to fabricate alumina spacers.

#### 3.4.2 Sample Electroding

A silk screen and squeegee fixture was obtained with a specified electrode pattern and guard ring. Sample insulator disks were lapped to a thickness of 10 and 30 mils and an imprint of the electrode pattern was squeegeed onto the sample surfaces. A commercial platinum paste was used.

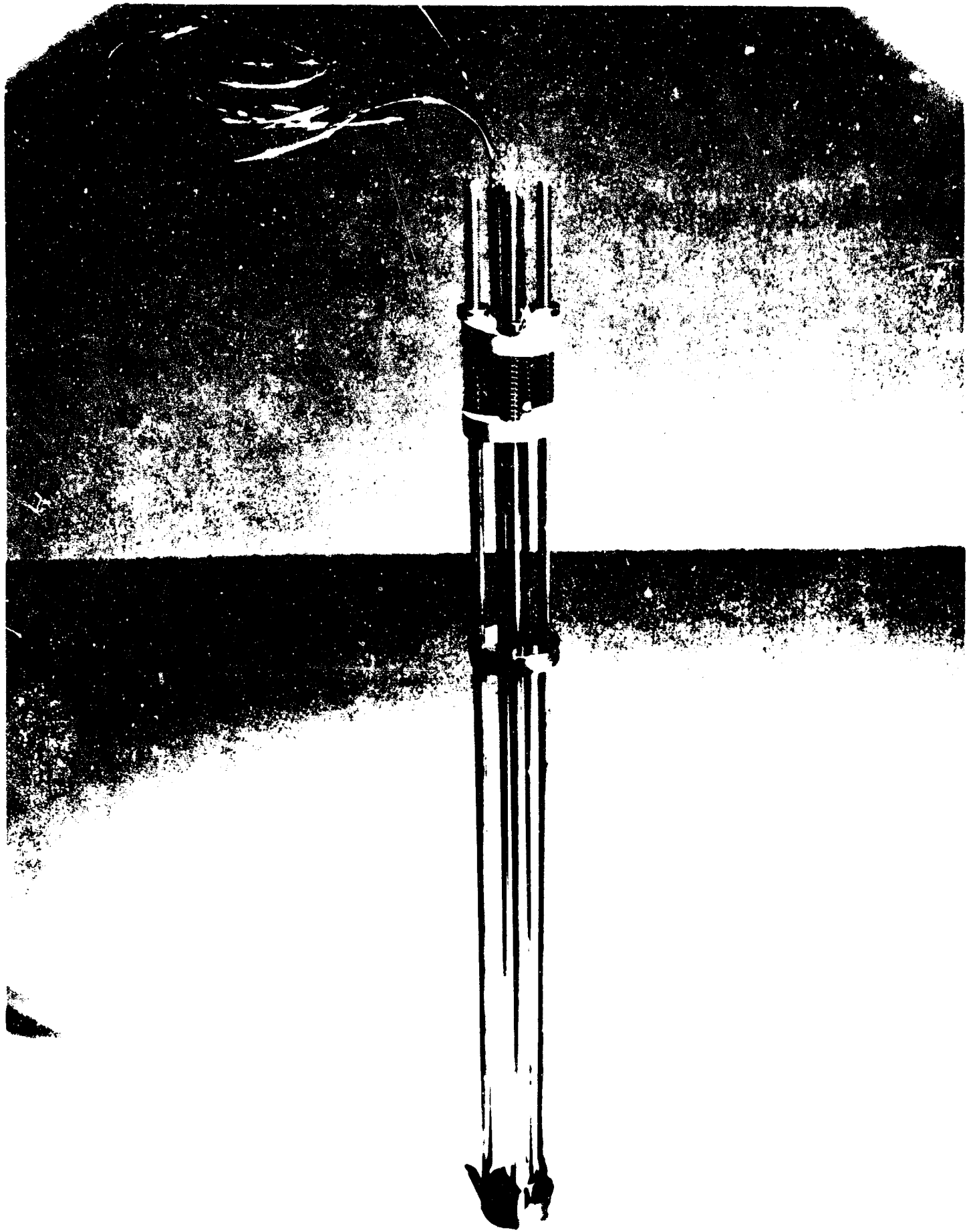


Figure 7. Spring Loaded Stainless Steel Fixture for Resistivity Measurements

The samples were then fired to 1000 C to burn out the organic vehicle in the platinum paste and to form adherent electrodes. Good electrode definition was obtained and it is planned to continue with these electroding techniques to produce samples for surface and volume resistivity measurements.

### 3.5 Plasma Sprayed Interlaminar Insulation

#### 3.5.1 Structure of High Purity $\text{Al}_2\text{O}_3$ and $\text{Y}_2\text{O}_3$ Coatings

Figures 8 through 13 show the microstructure of plasma sprayed Linde A (99.99  $\text{Al}_2\text{O}_3$ , 0.3 micron particle size) coatings on various Hiperco substrates. A number of coatings were made at different arc currents ranging from 100 to 650 amps in an effort to correlate arc current with coating characteristics and structure. Reference to Figure 8, for example, shows two distinct types of alumina particles. The whitish, opaque agglomerates obviously did not melt in the 100 amp plasma arc whereas the transparent, "pancake" shaped globules landed on the substrate in a molten state ( $> 2,000$  C). It is also evident that many of these molten droplets flattened out considerably on impact and immediately froze into a solid (diameters vary from 10 to 75 microns). It is estimated that the largest flattened droplets have diameter to thickness ratios greater than 40 to 1.

Figures 8 and 11 show quite clearly a number of smaller diameter and more spherically shaped droplets (ranging from about 5 to 10 microns in diameter). These particles did not possess sufficient mass and/or were not propelled at a high enough velocity to generate sufficient kinetic energy ( $1/2 mv^2$ ) to flatten into a pancake configuration.

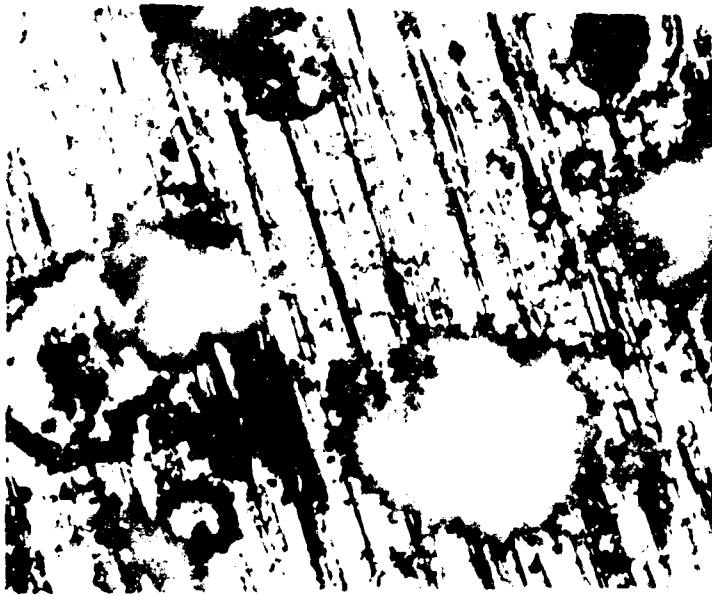


Figure 8. Plasma Sprayed  
Linde A on Hiperco,  
100 Amps Arc Cur-  
rent  
(500 X Magnification)

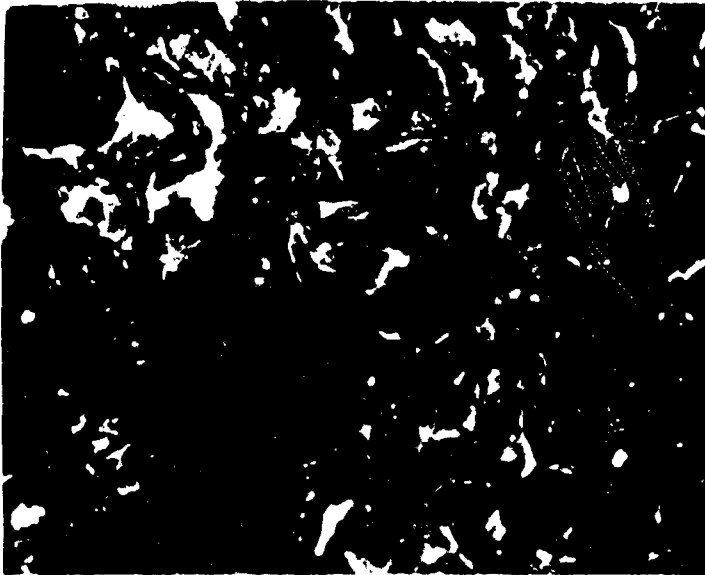


Figure 9. Plasma Sprayed  
Linde A on Hiperco,  
600 Amp Arc Cur-  
rent  
(500 X Magnification)



Figure 10. E Core Hiperco  
Lamination Sprayed  
Linde A at 600 Amps  
(500 X Magnification)



Figure 11. Plasma Sprayed Linde  
A - 650 Amp Arc  
Current  
(500 X Magnification)



Figure 12. Plasma Sprayed Linde  
A - 500 Amp Arc  
Current  
(1000 X Magnification)

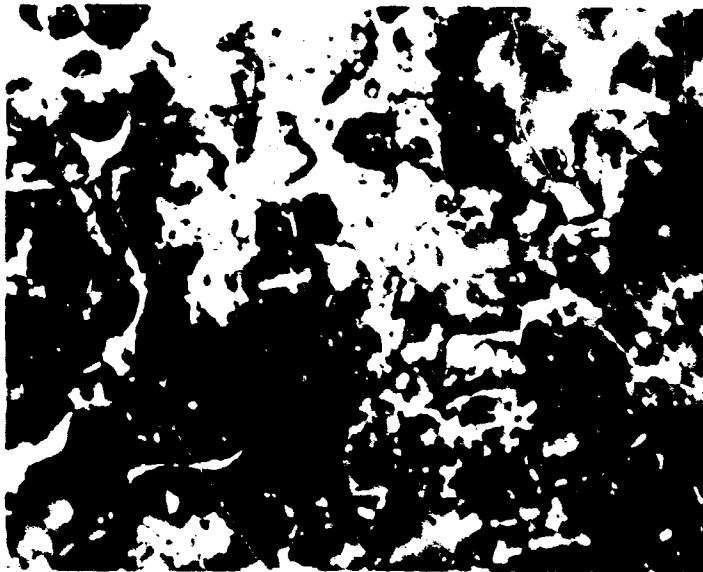


Figure 13. Yttrium Oxide Plasma  
Sprayed on E Core  
Hiperco at 600 Amps  
(500 X Magnification)

Figure 13 is a photomicrograph of yttrium oxide plasma sprayed at 600 amps. Although the figure does not clearly show the overall structure, viewing the specimen surface through a microscope and varying the focal point, shows that individual particles are more nearly spherical in shape. Yttrium Oxide has a higher melting point than  $Al_2O_3$  (Linde A) which might account for the comparative difference between the two structures. The surfaces of the yttrium oxide particles probably melted while the interior remained solid.

A plasma sprayed deposit made up of a series of laminated and flattened particles or droplets would probably result in a higher density coating.

The following observations and conclusions can be made regarding these experiments.

- 1) Plasma arc current (argon gas) in the range from 500 to 650 amperes results in the best overall coatings.
- 2) The population of unmelted alumina agglomerates increases markedly at low amperage (100 amperes).
- 3) At 650 amperes (max. obtainable) some unmelted agglomerates are in evidence. The agglomerates are composed of many 0.3 micron particles of  $Al_2O_3$ , indicating agglomeration has probably occurred before the powder enters the arc chamber. Even if the powder could be fed to the arc as individual 0.3 micron particles, it is questionable that all particles would be melted.

- 4) The particle size and distribution of oxide feed powders can have a significant effect on coating density, adherence and other physical and electrical properties.
- 5) It has been demonstrated that adherent and very thin ( $>1$  mil) alumina coatings can be applied to magnetic laminations by plasma spray techniques. Results also indicate that the effective thickness of these coatings can be further reduced without sacrificing electrical properties.
- 6) To accomplish the above, the following will be investigated.
  - a) Study oxide particles (feed powder) in the range from 1 to 40 microns.
  - b) Determine optimum powder feed rate at specific arc currents and gas flows.

### 3.6 Processed Insulators

#### 3.6.1 High Alumina Ball Mill

A photograph of a specially fabricated high alumina ball mill is shown in Figure 14. The mill lining consists of a 6 inch section of closed end alumina tubing four inches in diameter. This material (Triangle RR supplied by Morganite, Inc.) is reported to have an alumina content greater than 99.7%. Grinding media were fabricated by cutting a number of small cylinders from  $3/8$  and  $5/16$  inch diameter solid rods made from the same material as the lining.

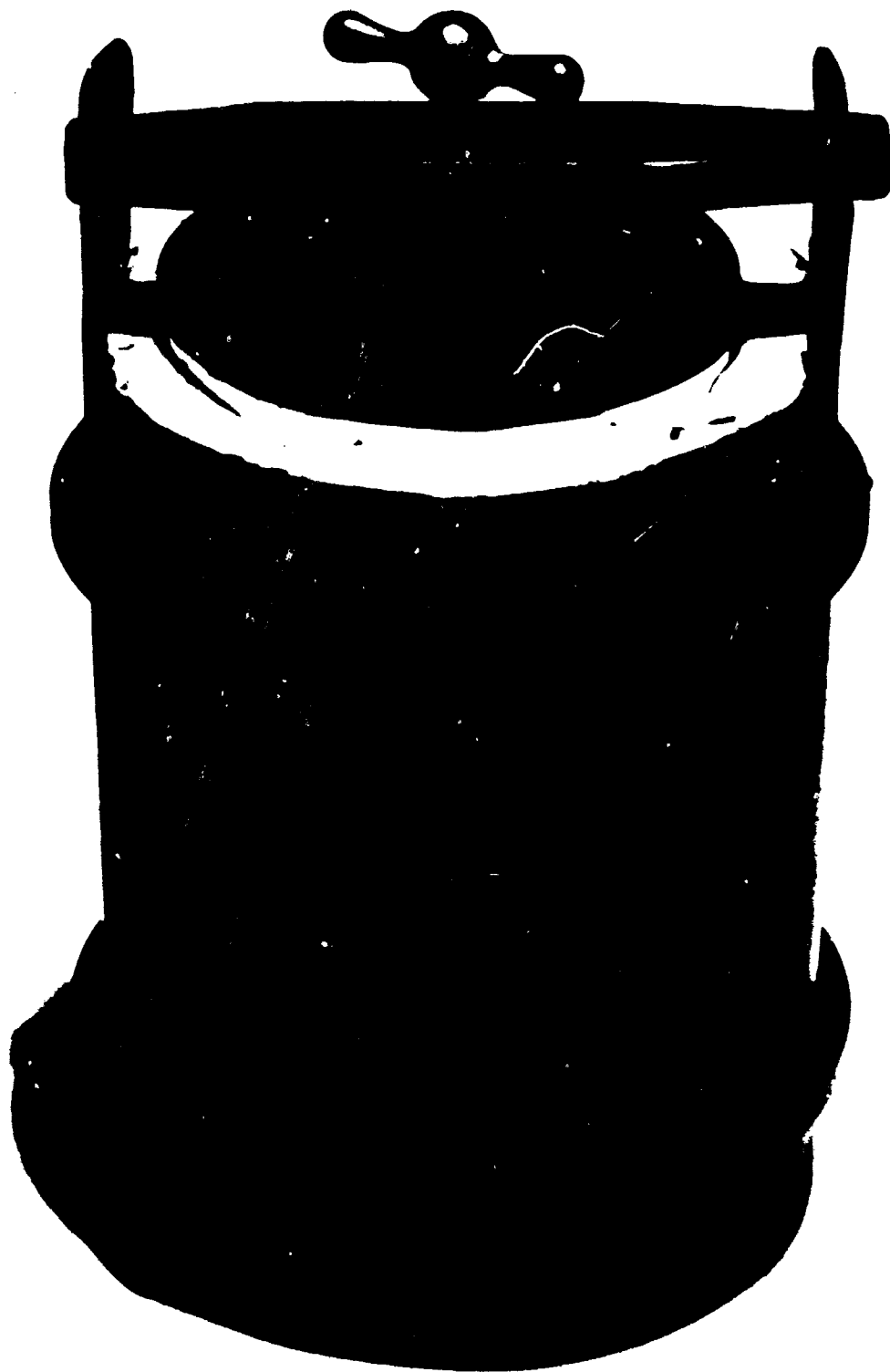


Figure 14. High Purity Alumina Ball Mill - Lining: Triangle RR  
(99.7%  $\text{Al}_2\text{O}_3$ )

Commercially available ball mills are usually made with an 80 - 90% alumina lining. The remaining 10 - 20% of the composition contains a large amount of silica. During a long milling operation, a small amount of the mill lining will be worn away and mixed with the charge. Silica, in particular, is an unwanted contaminant, since it can seriously reduce the alkali metal corrosion resistance of fired ceramics. (Reference Section 3.3.1.)

It is planned to use this 99.7% alumina mill to process most of the insulating materials, metallizing mixes and potting compounds requiring particle size reduction and/or intimate mixing and homogenization. An initial test was made to quantitatively determine the amount of silica pick-up from the mill during a prolonged milling schedule.

A 100 gram charge of -100, +325 mesh size alumina (specially processed Alite 610 material, Alite Division U.S. Stoneware) was placed in the mill together with distilled water and the grinding media. The mill rotated on a jar mill roller for approximately 90 hours. Figure 15 shows a 200 X magnification of the starting material. These particles are spherical in shape and measure between 0.004 and 0.001 inch in diameter. Figure 16 shows the same material at 200 X magnification after milling. Most of the particles appear to be less than 0.0005 inch across their widest dimension, indicating that at least an order magnitude reduction in size was achieved.

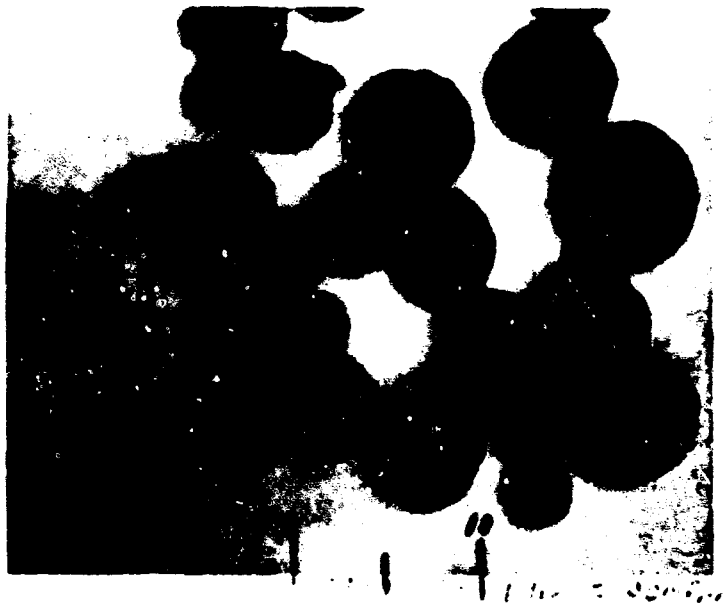


Figure 15. High Purity Alumina (Alite 610) Prereacted to Achieve Large Particle Size Material (-100, +325 Mesh) (200X Magnification)

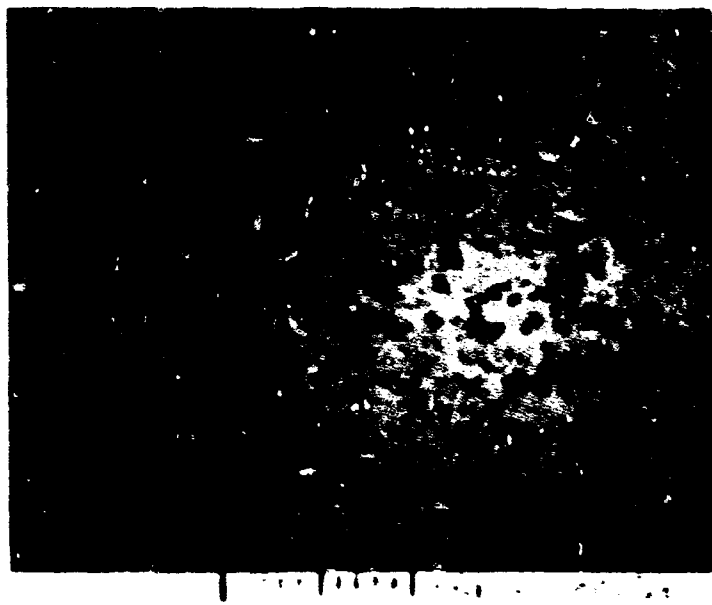


Figure 16. Same Material as Shown in Figure 15 Except Ball Milled for Approximately 90 Hours in Mill Shown in Figure 14 (200X Magnification)

A series of duplicate silicate analysis were made on the 90 hour milled material and the material, as received. Results show a total silica pick-up of about 200 ppm which is considered to be a negligible amount and may be within the limits of experimental error. A spectrographic analysis will be run to substantiate these results.

### 3.6.2 Inorganic Fluoride Insulation

Single crystal, alkaline earth fluorides were selected for initial testing in 850 C potassium vapor because of their purity and absence of grain boundaries and reported resistance to alkali metals. Polycrystalline and single crystal calcium fluoride, for example, has been found by several investigators (equation 5) to be resistant to sodium (liquid and vapor) at temperatures up to 1000 F. In fact, one investigation has shown that calcium fluoride coatings are unaffected by 1000 F exposure to liquid sodium.

Reference to the thermodynamic data compiled in Table II shows that a number of alkaline earth and rare earth fluorides have more negative free energies of formation than potassium fluoride (KF). These data correlate with the experimental observations previously referenced and offer guidelines for additional fluoride materials selection. A discussion on the use of free energy data to predict alkali metal stability of oxides can be found in Section 3.3.1.

Inorganic fluoride insulating materials offer a number of processing advantages primarily because they have lower melting points than oxides. Their resistance to potassium vapor, especially at temperatures of 850 C, has not been experi-

mentally demonstrated. If the tests in potassium vapor now in progress show that single crystals of alkaline earth fluorides are resistant to corrosion, an extensive program is planned to study this class of materials in more detail.

Fluoride materials would be candidates for interlaminar insulation and conductor insulation. They could be applied to magnetic materials and clad copper conductors at temperatures low enough to minimize any degradative effects on metal parts.

### 3.7 Pressure Sintered Ceramic-Metal Composites and Hermetic Seals

#### 3.7.1 Hot Pressing Rig

A hot pressing fixture has been constructed. Ultra high purity graphite (Speer Carbon Co.) was used to fabricate the die body and plungers. The die will be enclosed in a dense alumina tube with powdered insulation between the die and tube. A 20 KW R. F. generator has been installed and will be used to power a work coil surrounding the alumina tube. Sufficient R. F. energy should be available to inductively heat the graphite to any desired temperature up to and exceeding 2000 C. Provision will be made in the die body to optically measure temperatures, and argon gas will be introduced into the fixture to prevent excessive graphite oxidation.

The fixture will be placed on refractory brick and mounted within the framework of a 30 ton hydraulic press. This arrangement will permit pressures in excess of 10,000 psi to be applied to heated samples.

It is planned to use this equipment to prepare sintered and diffusion bonded hermetic seals. One approach that will be studied will be to simultaneously heat, under pressure, a series of concentric rings. These rings will be made of pre-pressed powdered metals (tungsten, columbium and zirconium, for example), mixtures of powdered metal and metal oxides, and pure oxides. If these techniques are successful, the final disk configuration would consist of an outer ring of sintered metal and an inner slug of metal separated and hermetically bonded to an insulating oxide.

Initially, it is planned to prepare test samples using several different powdered metals and ceramic oxides. Samples will be subjected to potassium vapor exposure at 850C and final materials selection will be based on the results of corrosion testing.

### 3.8 Ceramic to Metal Seals

The electrical terminal feed through seal for the electrical testing of materials including electric devices in potassium vapor at 600 - 850C is not commercially available. Part of this program was therefore devoted to obtaining a ceramic to metal seal resistant to 600 - 850C potassium vapor. A few of the approaches to solve this problem are listed below.

3.8.1 Active metal brazing using either zirconium titanium or combinations of both active metals alloyed with other metals, such as columbium, vanadium, iron and yttrium to obtain a lower melting brazing alloy. This alloy is then used to join the metal pieces of an electrical terminal seal to a high purity ceramic insulator.

3.8.2 Conventional molybdenum-manganese (80 - 20%) metallizing followed by a brazing material such as OFHC copper or palladium-cobalt to join the metallized ceramic to metal end pieces of an electrical terminal seal.

3.8.3 Vapor decomposition of a tungsten halide complex over the surface of a ceramic, such as alumina. The tungsten surface would then be brazed to seal metal pieces with nickel.

### 3.9 850 C Potassium Vapor Exposure - Active Metal Brazing Alloys

3.9.1 Ten active metal brazing alloys containing 15% zirconium and 50% titanium with the balance of material being columbium, iron and vanadium, in varying quantities, have been exposed to 850 C potassium vapors for 172 hours. Seven of the brazing alloys showed no attack by the potassium. Three of these alloys were brazed to pieces of Lucalox. The brazed Lucalox (99.8 Al<sub>2</sub>O<sub>3</sub>. 2% MgO) was exposed to 850 C potassium vapor for 172 hours. One of these brazing alloys stayed on the Lucalox and showed no visible signs of attack. This alloy is being used to fabricate terminal end electrical seals.

### 3.10 Magnetic Materials

#### 3.10.1 Materials Selection

The magnetic lamination materials selected for evaluation in the transformer are 0.008" Armco Ingot Iron, 0.008" Hiperco 27, 0.006" Cubex, 0.012" 5% aluminum iron, and 0.012" (3% Al, 1% Y) iron.

These materials were selected for the specific reasons described in the following discussion. The Armco Ingot Iron offers the advantage of low silicon and carbon and also low residual elements that might be attacked by potassium vapor. Its core loss properties are relatively poor but it has good magnetization properties. Cubex offers the advantage of a doubly-oriented lamination steel with excellent magnetic core loss properties. Cubex contains silicon that may be attacked by potassium vapor. The Hiperco 27 offers the advantage of cobalt in providing good magnetic permeability and also a high Curie point. This provides better elevated temperature magnetic properties. The 5% aluminum iron offers the advantage of  $Al_2O_3$  formation to prevent attack by potassium vapor and a high Curie point. The 3% Al - 1% Y iron alloy offers the advantage of yttrium in addition to aluminum in providing better corrosion resistance.

### 3.10.2 Magnetic Testing

Rowland rings were punched for magnetic test for evaluation from these materials, since the 2-1/4" I.D. x 2-3/4" O.D. rings used are better suited for high temperature magnetic testing (if required) than Epstein strips. Figure 17 shows the Rowland ring stacks.

For basic reference magnetic testing, the Rowland rings are insulated with 0.25 mil "Mylar" rings, an excellent interlaminar insulation that does not stress the surface of the laminations. These "Mylar" insulated Rowland ring tests will be compared to other insulation coatings such as plasma-arc sprayed Linde A. Correlation tests with other testing laboratories have been made to

ROWLAND RING  
PUNCHED LAMINATIONS

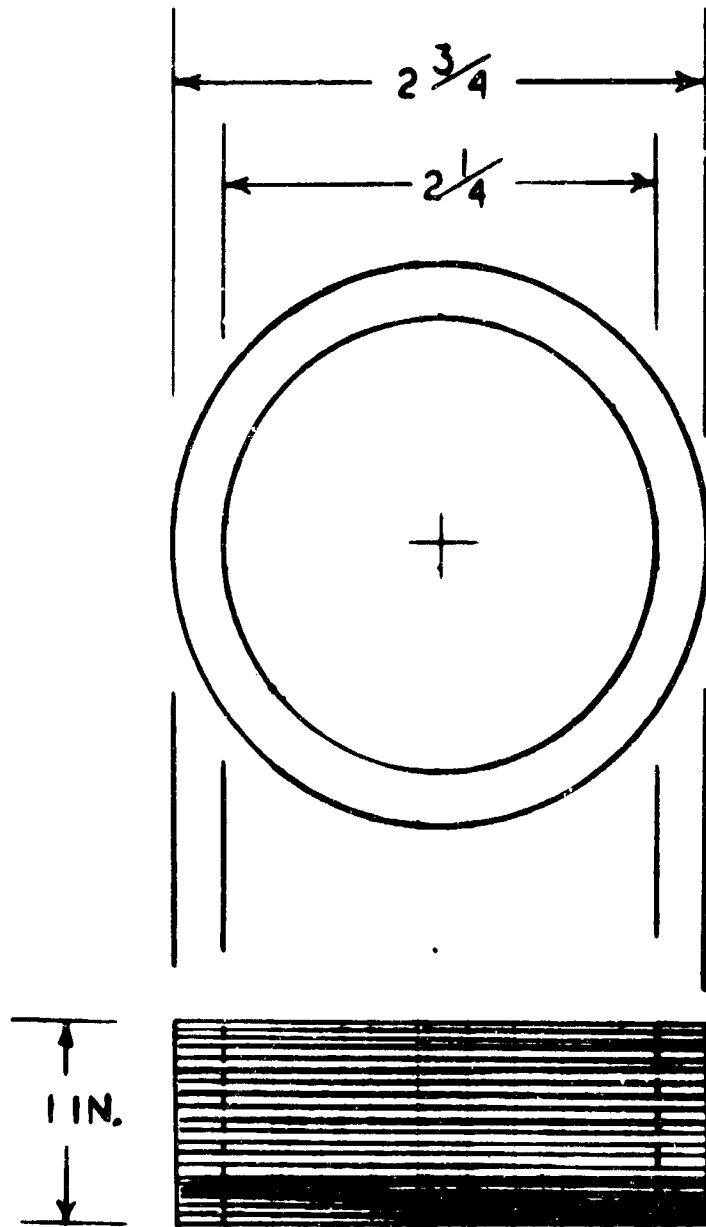


Figure 17. Rowland Ring Laminations used in Magnetic Testing

re-check the accuracy of our magnetic test equipment. These tests have shown very good correlation.

### 3.10.3 Preliminary Evaluation of Magnetic Tests

In Table IV, core loss separation data are shown. The plasma arc sprayed Linde A coating on Hiperco 27 shows that the insulation uniformity needs to be improved since the eddy current component is higher than the 0.25 mil Mylar insulated Hiperco 27. The Linde A coating of  $Al_2O_3$  shows good promise as an inter laminar insulation with high resistivity and good adherence. Theoretically, the coating will have good resistance to potassium vapor at elevated temperatures.

In Figures 18 through 25, the  $P_c$  total core loss and  $P_a$  apparent core loss, are shown. The comparative data for 400 cps at 80 KL/Sq. In. ( $\approx 12.4$ KG) for  $P_c$  and  $P_a$  are as follows:

Material	Insulation	$\frac{P_c}{\text{Watts/Lb.}}$	$\frac{P_a}{\text{Volt-Amps/Lb.}}$
0.008" Armco Ingot Iron	0.25 mil Mylar	23	30
0.006" Cubex	0.25 mil Mylar	7.8	16.5
0.008" Hiperco 27	0.25 mil Mylar	19.8	40
0.008" Hiperco 27	Linde A	21.2	54

These data indicate that 0.006" Cubex has the lowest  $P_c$  and  $P_a$  values. 0.008" Armco Ingot Iron has the highest  $P_c$ ;  $P_a$  values are higher than Cubex but lower than Hiperco 27.

TABLE IV

Core Loss Separation Data

Material	Insulation	Frequency cps	Core Loss, Watts/Lb. at B - Kilogauss					
			10KG			15KG		
			P <sub>c</sub> *	P <sub>e</sub> *	P <sub>h</sub> *	P <sub>c</sub> *	P <sub>e</sub> *	P <sub>h</sub> *
0.008" Armco Ingot Iron	0.25 mil Mylar	300	9.50	4.89	4.61	21.14	11.16	9.98
"	"	400	14.83	8.69	6.14	33.14	19.84	13.30
0.008" Hiperco 27	0.25 mil Mylar	300	9.4	2.86	6.54	18.0	5.65	12.35
"	"	400	13.8	5.08	8.72	26.5	10.03	16.47
"	Linde A	300	10.16	3.56	6.60	19.32	7.28	12.04
"	"	400	15.13	6.33	8.80	28.99	12.93	16.06
0.006" Cubex	0.25 mil Mylar	300	3.50	0.71	2.79	6.86	4.37	2.49
"	"	400	4.97	1.25	3.72	11.08	7.76	3.32

\*P<sub>c</sub> - Total Core Loss

P<sub>e</sub> - Eddy Current Loss

P<sub>h</sub> - Hysteresis Loss

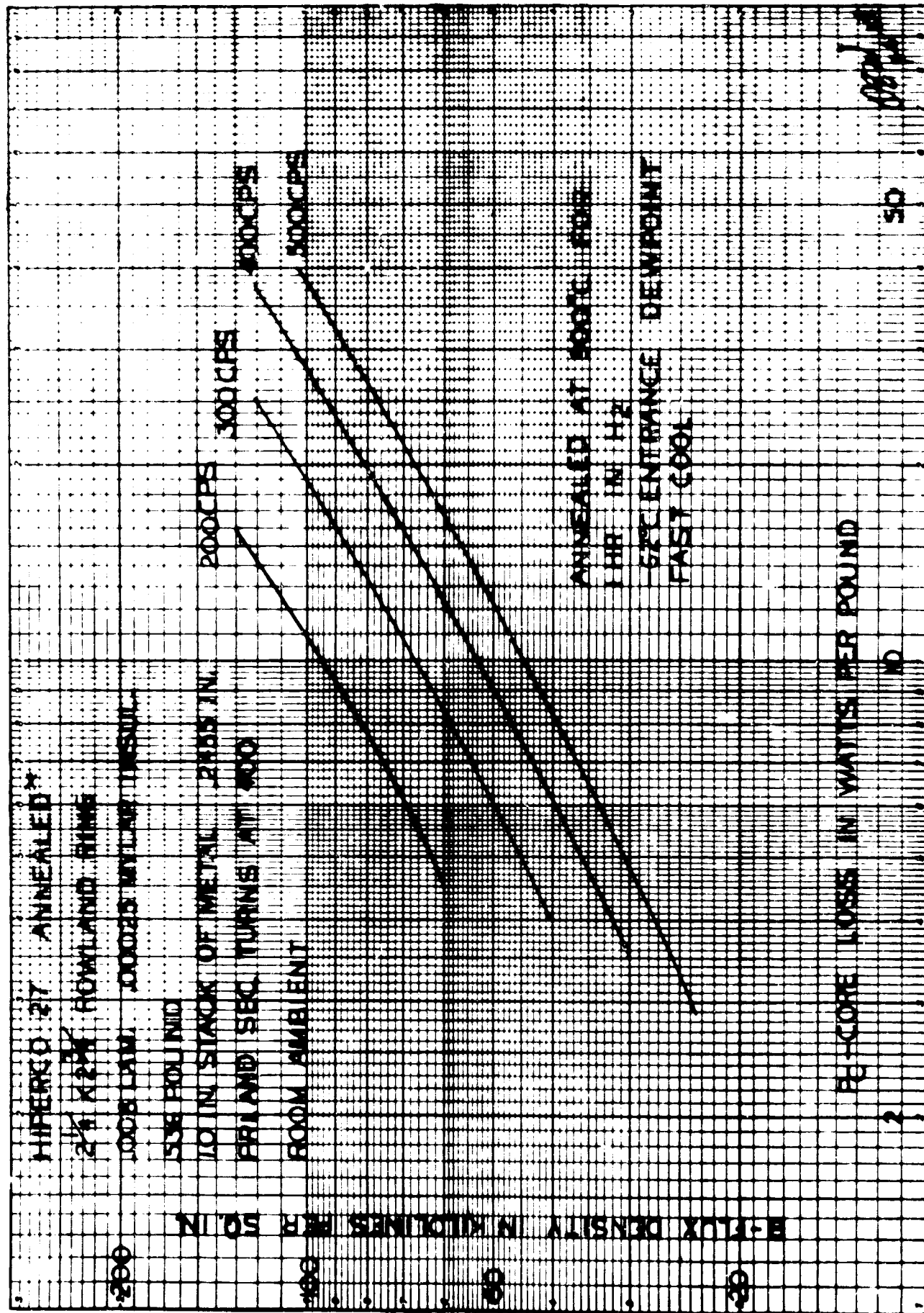
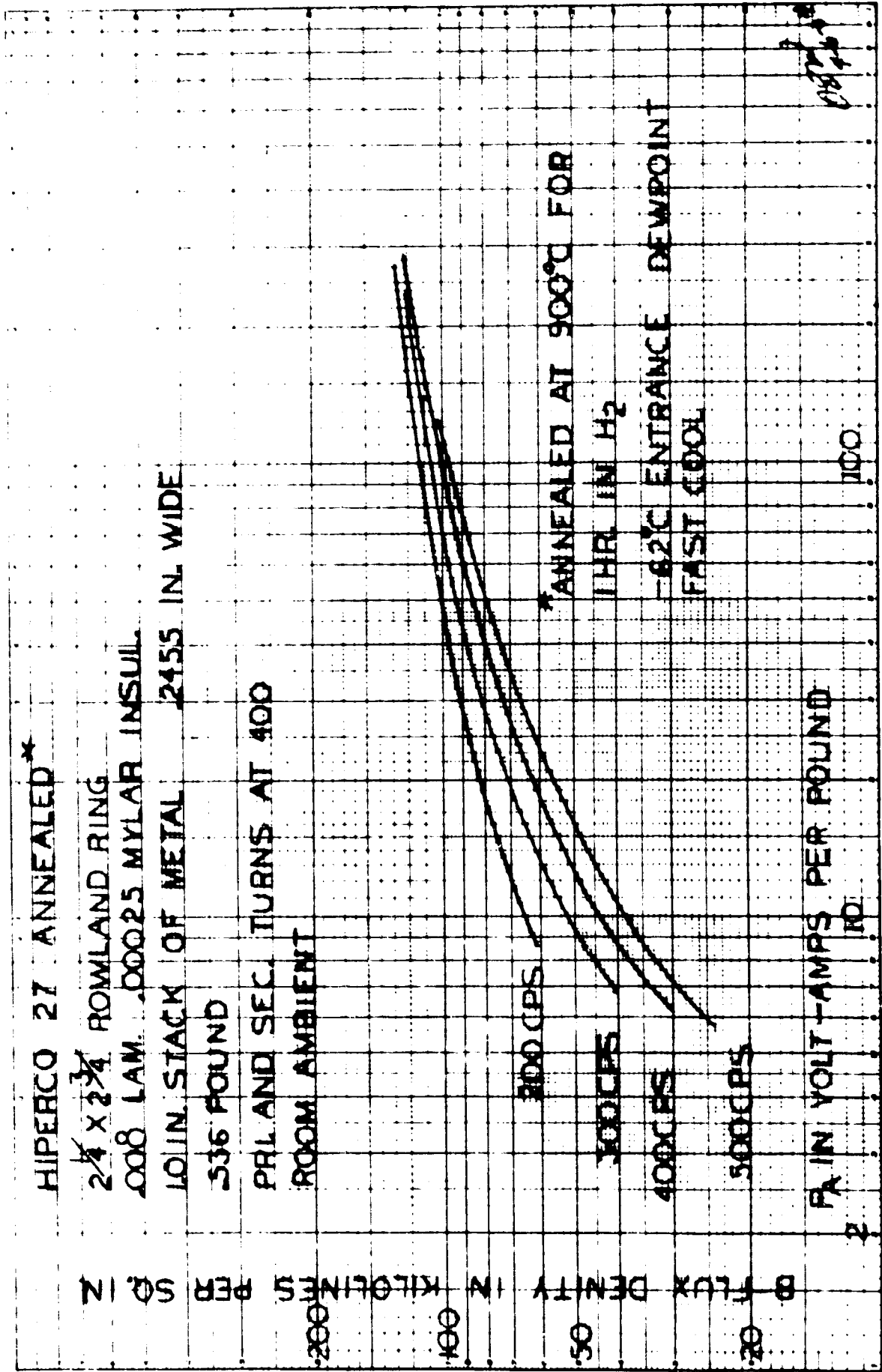


Figure 18. Core Loss of 0.008" Hiperco 27, Mylar Insulated



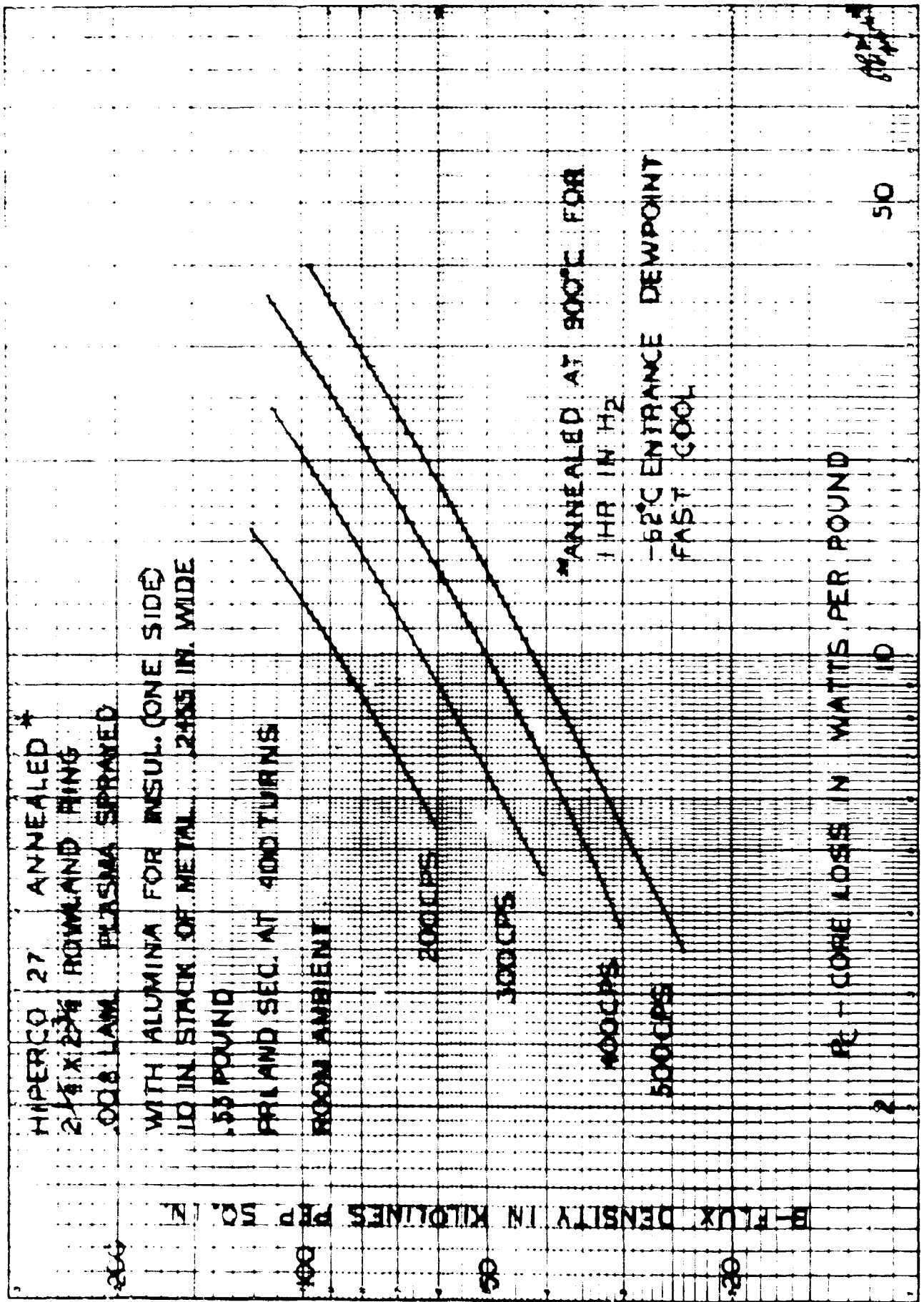


Figure 20. Core Loss of 0.008" Hipercro 27, A12O3 (99.997) Insulated

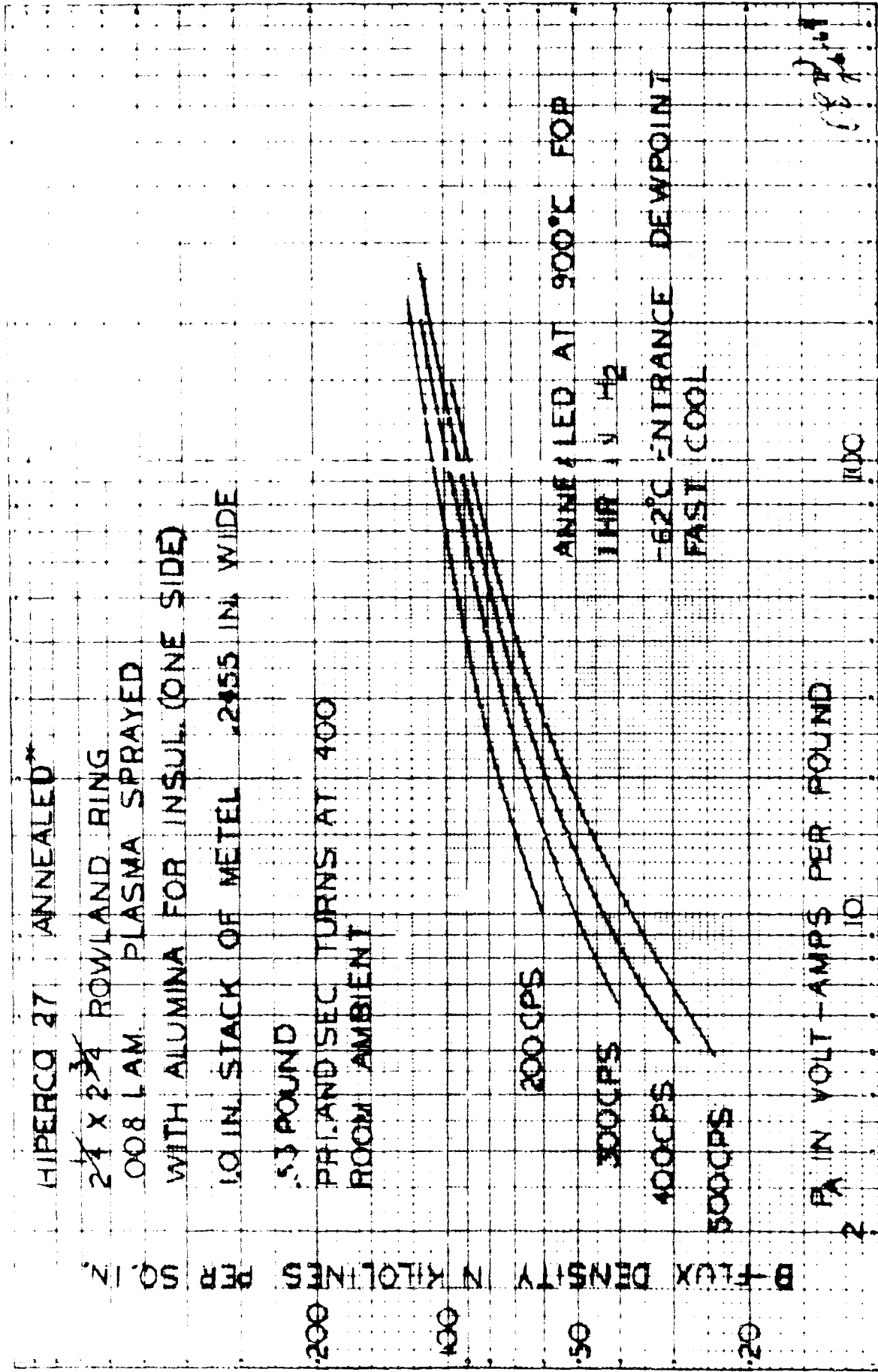


Figure 21. Apparent Core Loss 0.008" Hipercoco 27, A1203 (99.99%) Insulated

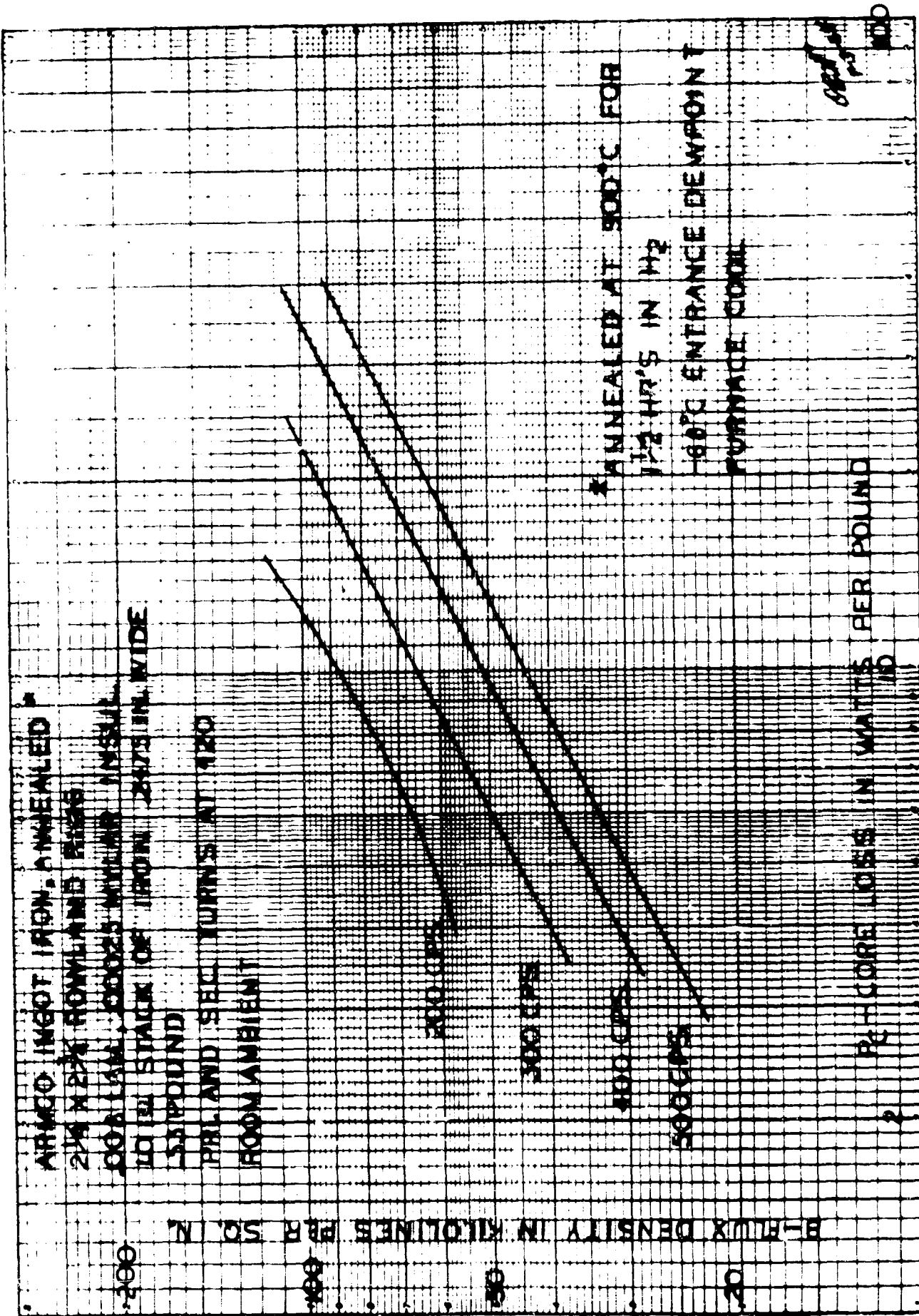


Figure 22. Core Loss of 0.008" Armco Ingot Iron. Mylar Insulated

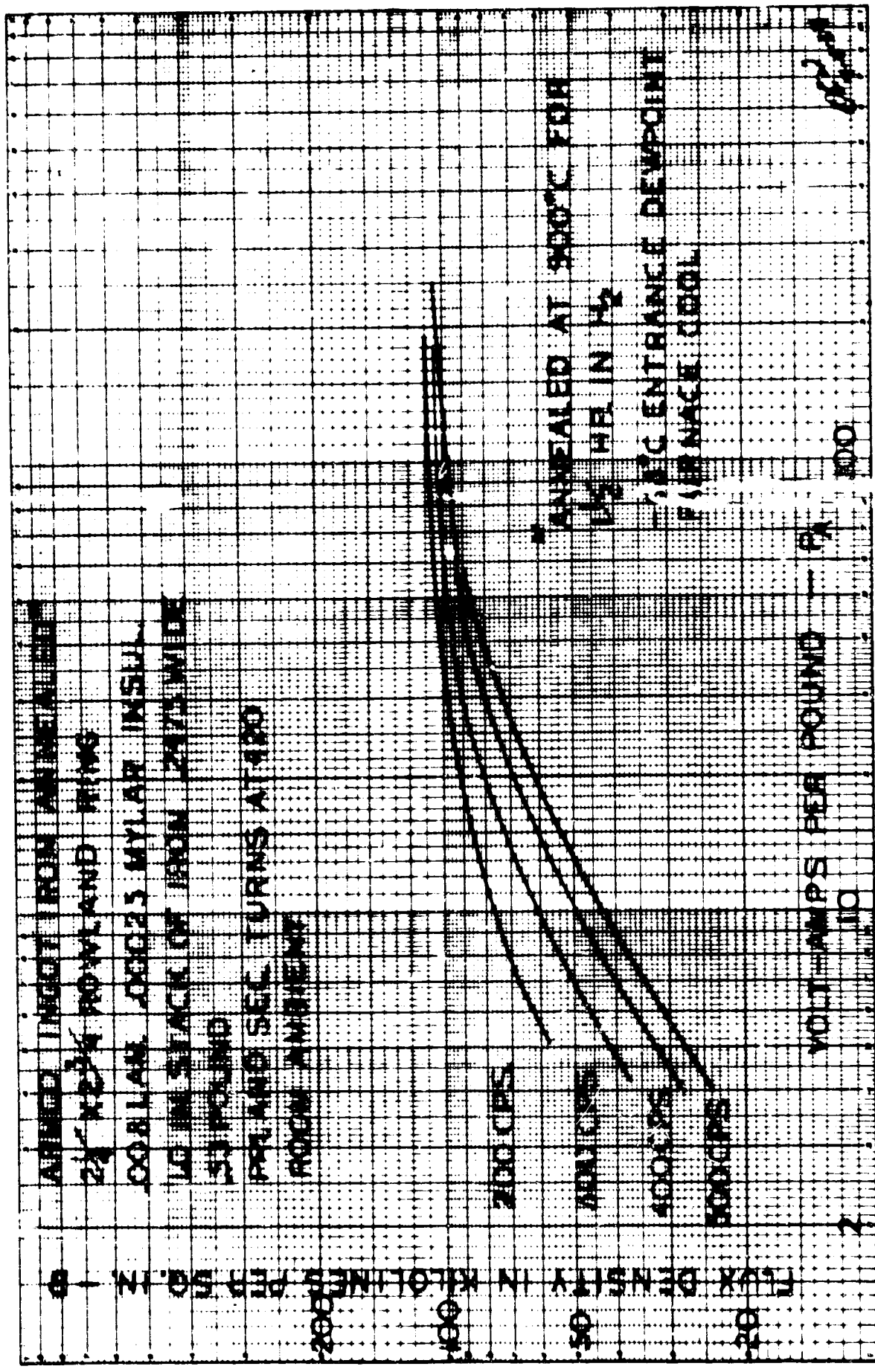


Figure 23. Apparent Core Loss of 0.008" Armco Ingot Iron, Mylar Insulated

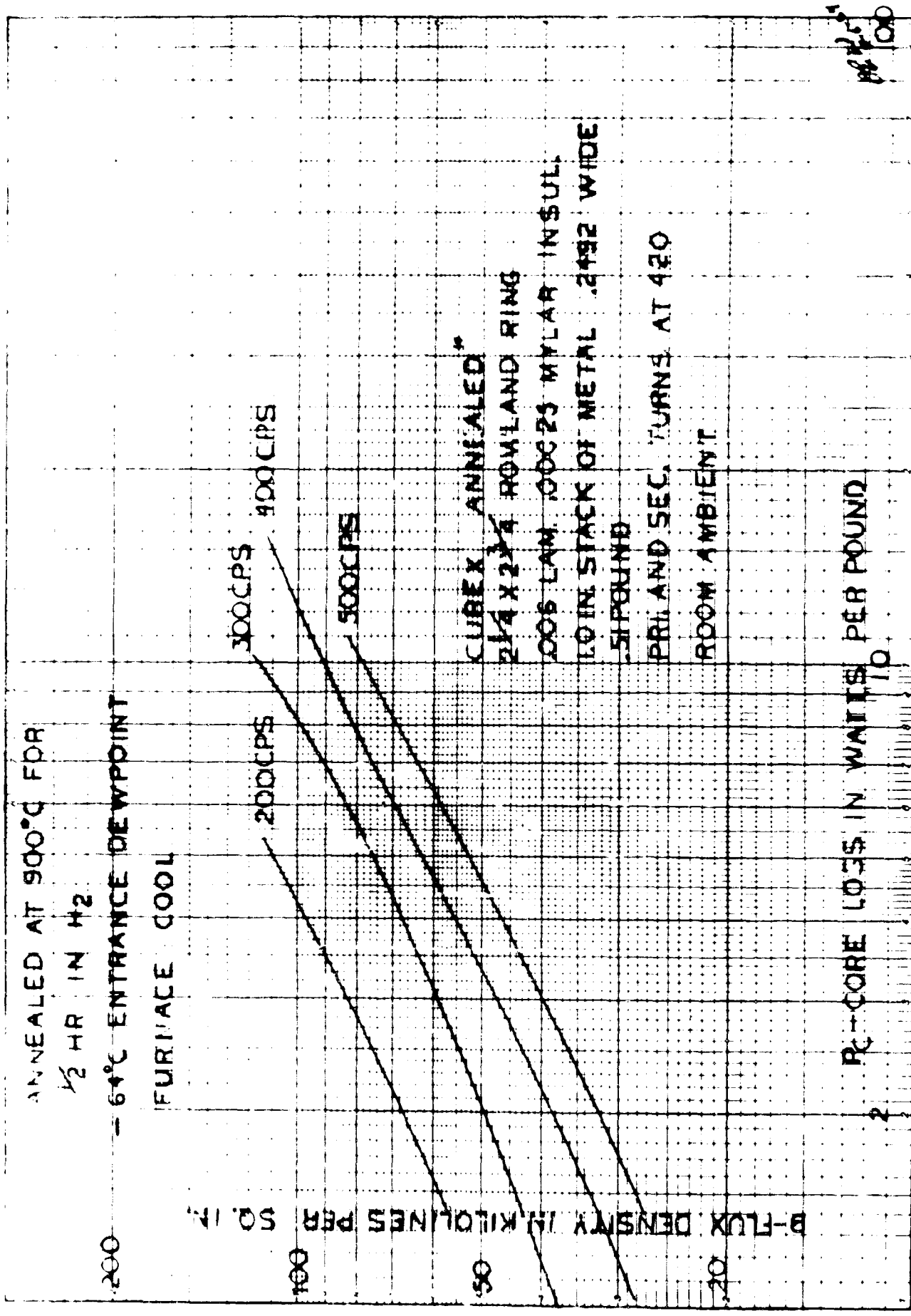


Figure 24. Core Loss of 0.006" Cubex, Mylar Insulated

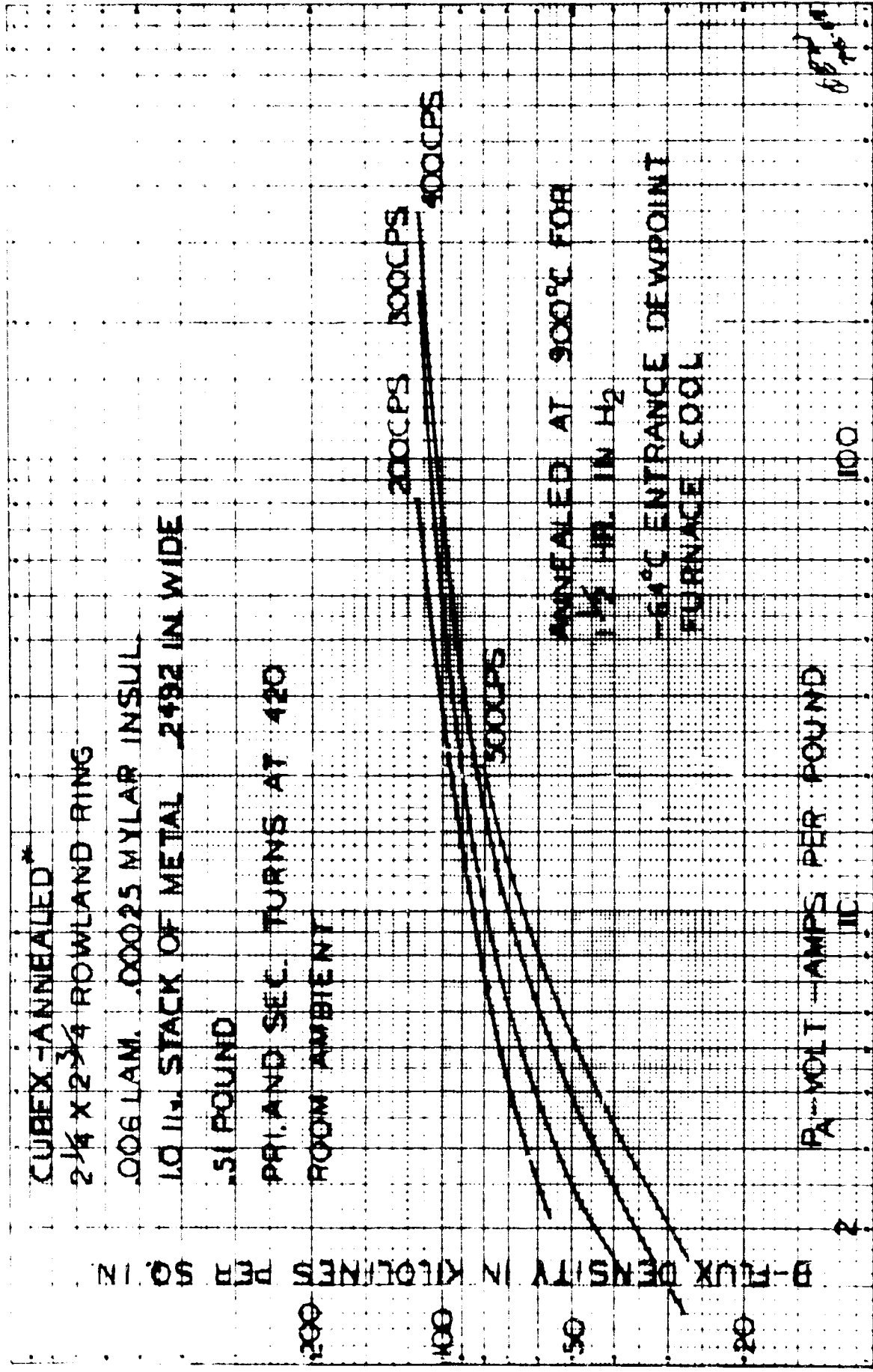


Figure 25. Apparent Core Loss of 0.006" Cubex, Mylar Insulated

### 3.11 Special Transformer

#### 3.11.1 Description and Design

The lamination design has been completed for all test transformers. The wire sizes have also been chosen for the primary and secondary windings. Primary windings will be No. 22 AWG and the secondary winding will be No. 6 AWG.

A transformer has been designed, using the concept of grooved ceramic coil forms made to slip over each other until the desired number of turns is obtained. Figure 26 shows two views of the transformer drawn to actual size. The first ceramic grooved insulator is shown in Figure 27. A clad conductor is shown wound in the grooves to more clearly illustrate transformer windings. Coil form measurements are given in Figure 28 for the complete set of primary and secondary forms. Ten coil forms will be needed for the primary (~ 550 turns of No. 22 AWG clad conductor). One coil form (~6 turns of No. 6 AWG clad conductor) will be used for the secondary. The first conductor used to make these windings will be nickel clad silver. The windings of this transformer will be bare of insulation in one fabrication and plasma-arc sprayed with sub-micron particle size (99.9%) alumina in another. Exposing the conductor bare and insulated will give potassium vapor corrosion data on cladding and insulation plus cladding.

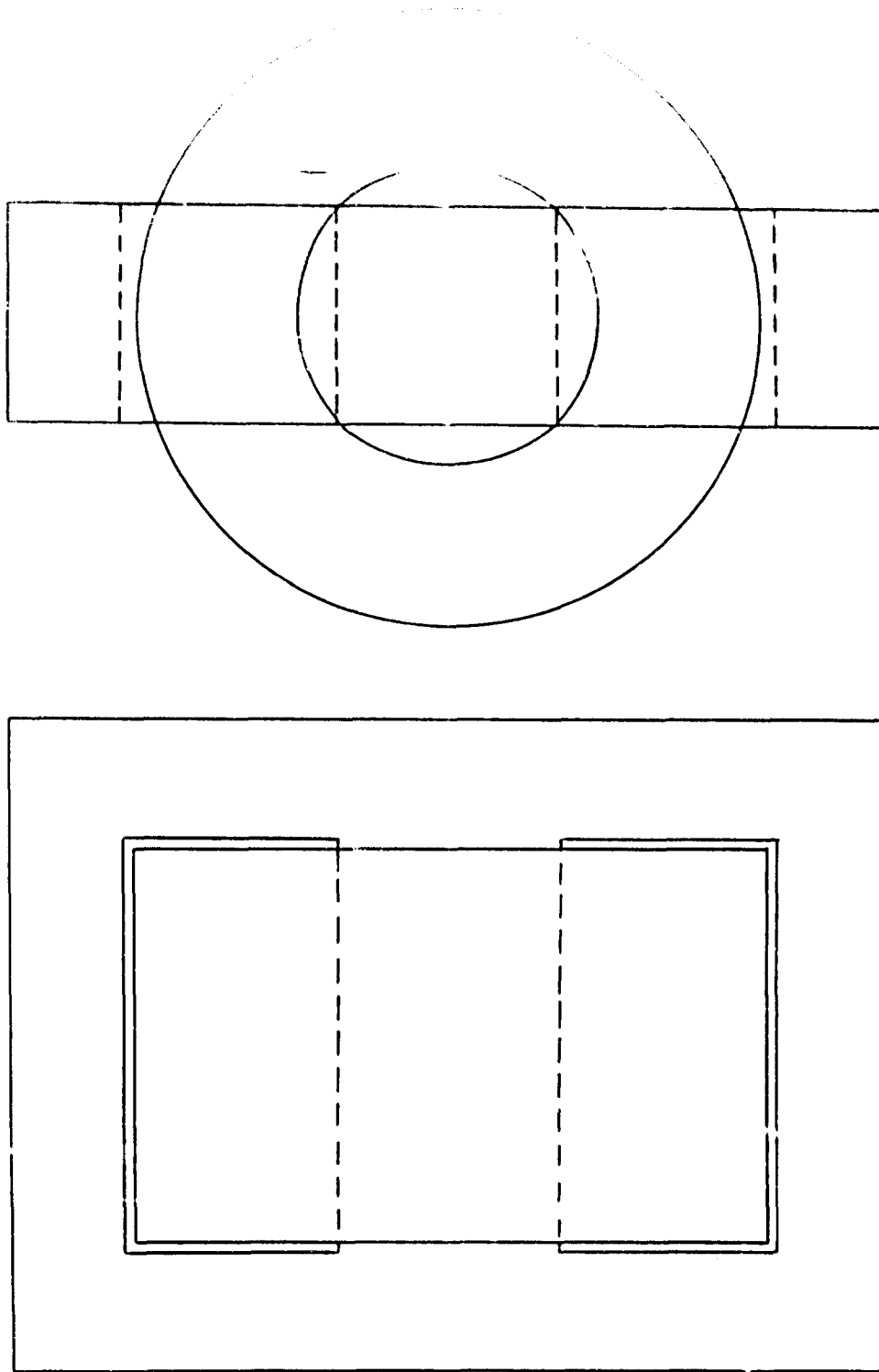
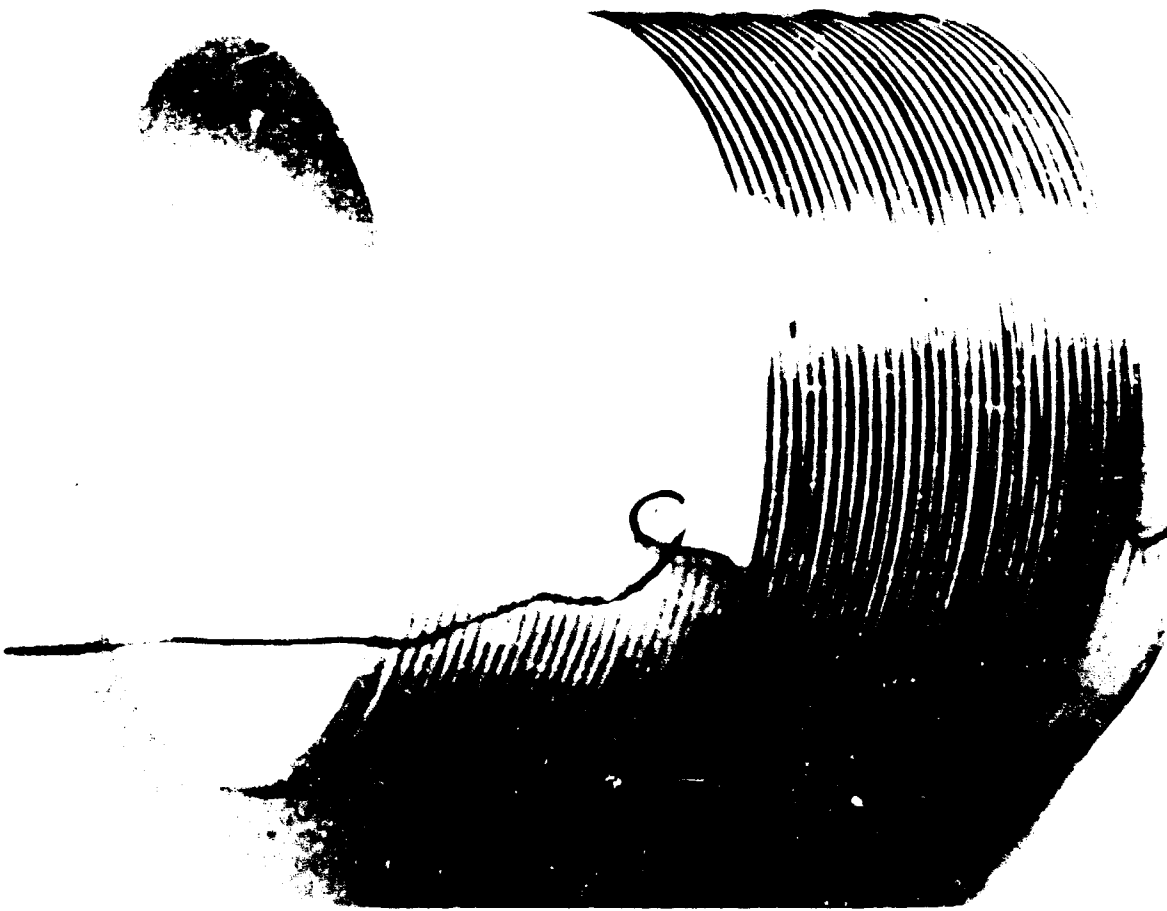


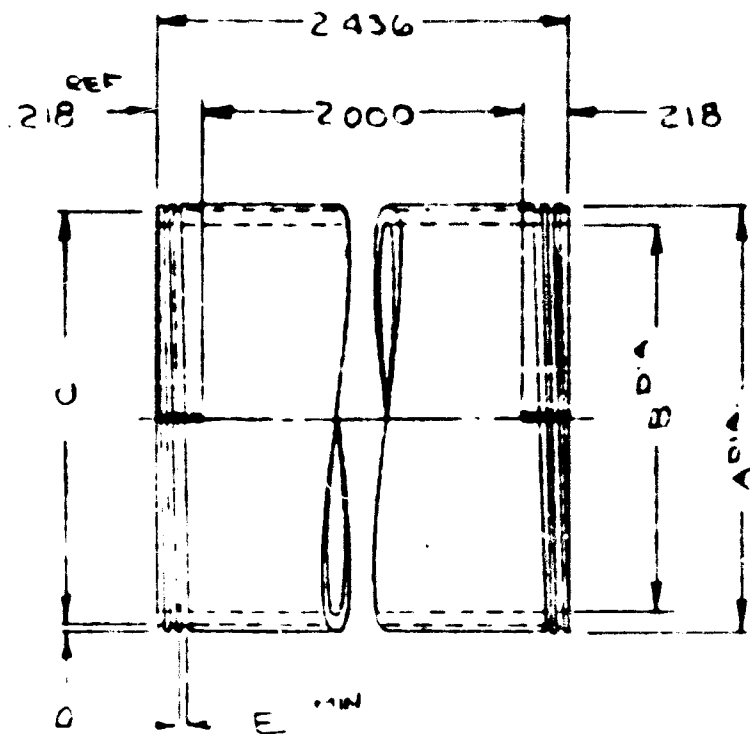
Figure 26. Top and End View of Special Transformer using Ceramic Spool Insulators of Alite A-610 Material (Actual Size)



**PART NO.**

**8/2**

Figure 27. Ceramic Ground Insulator Made of ALITE A-610 (99.0%  $Al_2O_3 \cdot 17 MgO$ )



	COIL FORM NO.										
	1	2	3	4	5	6	7	8	9	10	11
OUTSIDE	2.001	2.141	2.281	2.421	2.561	2.701	2.841	2.981	3.121	3.261	3.401
DIA "A"	1.999	2.139	2.279	2.419	2.559	2.699	2.839	2.979	3.119	3.259	3.399
INSIDE	1.862	2.002	2.142	2.282	2.422	2.562	2.702	2.842	2.982	3.122	3.262
DIA "B"	1.866	2.006	2.146	2.286	2.426	2.566	2.706	2.846	2.986	3.126	3.266
ROOT DIA	1.947	2.087	2.227	2.367	2.507	2.647	2.787	2.927	3.067	3.207	3.347
"C"	1.931	2.071	2.211	2.351	2.491	2.631	2.771	2.911	3.051	3.191	3.331
GROOVE	.026	.026	.026	.026	.026	.026	.026	.026	.026	.026	.163
DEPTH "D"	.034	.034	.034	.034	.034	.034	.034	.034	.034	.034	.171
GROOVE	.026	.026	.026	.026	.026	.026	.026	.026	.026	.026	.163
WIDTH "E"	.026	.026	.026	.026	.026	.026	.026	.026	.026	.026	.163

Alite Division U. S. Stoneware Co., Orrville, Ohio

Figure 28. Ceramic Coil Form Measurements

#### IV.

#### PROGRAM FOR NEXT QUARTER

##### 4.1 Potassium Vapor Corrosion Effects

More corrosion test samples will be exposed to potassium vapor.

Electrical terminal seals will be joined to corrosion test capsules for electrical tests in potassium vapor.

##### 4.2 Magnetic Materials

The magnetic materials, Hiperco 27, Armco Ingot Iron, and Cubex will be exposed to 600 C potassium vapor and examined for changes in magnetic properties, surface corrosion, and crystal changes.

##### 4.3 Conductors

Columbium clad Cu Fo, silver, and zirconium copper will be obtained in a 20-28 volume percent cladding. These conductors will be exposed to potassium at 850 C.

The electrical resistivity of the 70% columbium clad conductors shows the 20 - 28% columbium clad conductor will be within the 150% resistivity of OFHC copper at temperature. The calculated resistivity of 70% columbium clad silver is in the range of the observed value at 1562 F; therefore, it can be assumed the calculated

and observed values of a 20 - 28% columbium clad conductor will be within the 150% range. Resistivity measurements will be conducted on the 20 - 28% columbium clad conductors as a control measure.

#### 4.4 Ceramic Materials

The fluoride ceramics will be examined after their exposure to potassium vapor for attack. Eutectic mixtures of calcium fluoride and strontium fluoride will be cast into potassium corrosion test samples. These samples will be exposed to 850 C potassium vapor.

#### 4.5 Transformer Fabrication

The special ceramic spool transformer will be wound and checked if the ceramic spools are available. The conductor and lamination have been obtained but the ceramic insulators have not been received to date.

#### 4.6 Plasma-Arc Spraying of Ceramics

Sub-Micron size alumina (99.9%) will be applied to Hiperco 27 for interlaminar insulation. Clad conductors will be plasma sprayed with alumina or yttria while they are being wound on a ceramic spool.

V.

## REFERENCES

- (1) H. Humenck, Jr., W.D. Kingery, Metal Ceramic Interactions: III Surface Tension and Wettability of Metal - Ceramic Systems, J. Am. Cer. Soc., Vol. 37, No. 1, 1954
- (2) W. M. Armstrong et al, Interface Reactions Between Metals and Ceramics: I Sapphire - Nickel Alloys, J. Am. Cer. Soc., Vol. 45, No. 3, 1962
- (3) H. F. Tripp, B. W. King, Thermodynamic Data on Oxides at Elevated Temperatures, J. Am. Cer. Soc., Vol. 38, No. 12, 1955
- (4) A. Glassner, The Thermochemical Properties of Oxides, Fluorides, and Chlorides to 2500 K, ANL - 5750, 1957
- (5) C. A. Elyard, H. Rawson, The Resistance of Glasses of Simple Composition to Attack by Sodium Vapor at Elevated Temperatures, Advances in Glass Technology, Plenum Press, N. Y., 1962

- (6) L. Reed, Spur Phase III, Westinghouse Quarterly Report (AF33-657-109-22), May 17 - August 25, 1963 by Eitel-McCullough, Inc., Device Research Laboratory.
- (7) E. S. Baber et al, Alkali Metal Resistant Wire, Report No. APL-TDR-64-42 by Westinghouse Electric Corp. under AF33(657) 10701, April 15, 1964.

APPENDIX A

CALCULATION OF CONDUCTIVITY FROM WEIGHT

PERCENTAGES OF CLAD WIRES

$$PC_{VI} = \frac{PC_{WI} \times \delta_A}{PC_{WI} \times \delta_A + PC_{WA} \times \delta_I} \times 100 \quad (1)$$

$$PC_{VA} = \frac{PC_{WA} \times \delta_I}{PC_{WA} \times \delta_I + PC_{WI} \times \delta_A} \times 100 \quad (2)$$

$$\rho_T = \frac{\rho_A \rho_I \times 100}{\rho_A \times PC_{VI} + \rho_I \times PC_{VA}} \quad (3)$$

$$\text{IACS Conductivity} = \frac{\rho_c}{\rho_T} \times 100 \quad (4)$$

$$= \frac{\rho_c [\rho_A \times PC_{VI} + \rho_I \times PC_{VA}]}{\rho_A \rho_I} \times 100 \quad (5)$$

$$= \rho_c \left[ \frac{PC_{VI}}{\rho_I} + \frac{PC_{VA}}{\rho_A} \right] \times 100 \quad (6)$$

$$= \rho_c \left[ \frac{PC_{WI}}{\rho_I} \left( \frac{\delta_A}{PC_{WI} \delta_A + PC_{WA} \delta_I} \right) + \frac{PC_{WA}}{\rho_A} \left( \frac{\delta_I}{PC_{WI} \delta_A + PC_{WA} \delta_I} \right) \right] \times 100 \quad (7)$$

$$= \frac{\rho_c}{PC_{WI} \delta_A + PC_{WA} \delta_I} \left( \frac{PC_{WI} \delta_A}{\rho_I} + \frac{PC_{WA} \delta_I}{\rho_A} \right) \times 100 \quad (8)$$

$$= \frac{\rho_c}{\rho_I \rho_A} \left[ \frac{\rho_A PC_{WI} \delta_A + \rho_I PC_{WA} \delta_I}{PC_{WI} \delta_A + PC_{WA} \delta_I} \right] \times 100 \quad (9)$$

## APPENDIX A (Cont.)

### Calculation of Conductivity from Weight Percentage of Clad Wire

$PC_{V1}$	=	Percent cladding by volume
$PC_{VA}$	=	Percent core material by volume
$PC_{W1}$	=	Percent cladding by weight
$PC_{WA}$	=	Percent core material by weight
$\delta_A$	=	Density of core material in g/CC
$\delta_I$	=	Density of cladding in g/CC
$\rho_1$	=	Resistivity of cladding in microhm-CM
$\rho_A$	=	Resistivity of core in microhm-CM
$\rho_T$	=	Resistivity of clad wire in microhm-CM
$\rho_c$	=	Resistivity of copper at 1562 F in microhm-CM

#### Calculated Percent IACS Conductivity

28% Columbium Clad Silver = 78.19%

70% Columbium Clad Silver = 41.19T